malization of liver function, improvement of hepatic inflammation and fibrosis and a decreased risk of the development of hepatocellular carcinoma [2,3]. The problem is that only 50% of patients achieve a sustained virological response (SVR) to therapy even with the most highly developed regimens of IFN [4,5]. The remaining patients who fail to clear the virus are left with the risk of progressive disease. In order to halt this potentially progressive disease, there is a need to establish an effective target of therapeutic intervention independent of antiviral therapy. Therefore, it is important to define risk factors for the progression of fibrosis among chronic hepatitis C patients who do not achieve a SVR to IFN therapy.

Several factors that may affect the rate of progression of fibrosis have been investigated extensively, including older age at infection, male gender, obesity, heavy alcohol consumption, and a high grade of necroinflammation [6–8]. Several cross-sectional and longitudinal studies suggest that hepatic steatosis, which is a common histological feature of chronic hepatitis C [9], influences the progression of hepatic fibrosis [10–14], while other studies did not find such an association [15–18]. Besides these conflicting results, no study to date has reported the effect of steatosis on longitudinal progression of fibrosis among patients who fail to respond to IFN therapy. Therefore, we studied factors associated with progression of fibrosis in those who failed IFN therapy by comparing paired pre-treatment and post-treatment liver biopsies.

2. Methods

2.1. Patients

The aim of the study was to identify risk factors associated with progression of fibrosis in chronic hepatitis C patients who failed to achieve a SVR to IFN therapy. To be included in this retrospective study, patients had to have undergone liver biopsy before and after therapy, been treated with IFN and not achieved a SVR. Patients with alcohol consumption of more than 20 g per day, co-infected with HBV or HIV, and those with another known aetiology of liver disease, such as autoimmune hepatitis or metabolic disorders, were excluded. A database of patients who had undergone liver biopsy at Musashino Red Cross Hospital between 1990 and 2004 was reviewed retrospectively and a total of 1241 chronic hepatitis C patients treated with IFN were identified; of these, 407 had a SVR and 834 had not achieved a SVR. Among those with treatment failure, 104 fulfilled the above criteria but seven patients with cirrhosis before treatment were excluded because the endpoint of the study was progression of fibrosis. Therefore, this study cohort consisted of 97 patients. In these patients, second liver biopsies were performed before the second course of IFN therapy. Otherwise, there were no standardized indications for the second liver biopsy which may be the limitation of our study. Demographic characteristics of patients at the time of initial biopsy are shown in Table 1. The time between the paired biopsies was 5.9 years on average, with a range of 1.2–11.6 years. The median interval between first biopsy and IFN therapy was 3 days (range 2–93 days), and that between completion of IFN therapy and second biopsy was 5.4 years (range 0.8–11.2 years). Laboratory tests were performed monthly or bimonthly in all patients and all measurements were taken at our single hospital.

Table 1
Demographic characteristics of patients

Number of patients	97
Age (years)	52 ± 9
Gender: male/female	50/47
BMI (kg/m^2)	23.9 ± 3.2 (median 24.0, range19–33)
BMI <25/25–30/30 ⩽ (kg/m^2)	55/37/5
Route of transmission	
Blood transfusion/unknown	38/59
Duration of infection (years)	30.4 ± 9.2 (median 33.5, range 3–48)
Genotype 1b/2a/2b	85/4/8
Serum HCV-RNA (Meq/ml)	7.7 ± 9.7
Pretreatment AST (IU/l)	73 ± 40
Pretreatment ALT (IU/l)	104 ± 69
Pretreatment GGT (IU/l)	51 ± 44
Histological variables at first biopsy	
Stage of fibrosis 1/2/3	33/38/26
Grade of activity 0/1/2/3	15/36/41/5
Grade of steatosis 0/1/2/3	21/37/25/14
Size of steatosis macro/micro/mixed	16/17/64
Localization of steatosis centrilobular/diffuse	3/94

BMI, body mass index; AST, aspartate aminotransferase, normal range is 7–38 IU; ALT, alanine aminotransferase, normal range is 4–43 IU/l; GGT, gamma-glutamyltransferase, normal range is 0–73 IU/l; macro, macro-vesicular steatosis; micro, micro-vesicular steatosis.

2.2. Histological evaluation

Median length of biopsy specimen and number of portal tracts were 13.0 mm (range 10–40 mm) and 12 (range 6–34). All liver biopsy specimens were evaluated separately by three independent pathologists who were blinded to the clinical data. If there was discordance, the scores assigned by two pathologists were used for the analysis. Fibrosis and activity were scored according to the METAVIR scoring system [19]. Fibrosis was staged on a scale of 0–4: F0 (no fibrosis), F1 (mild fibrosis: portal fibrosis without septa), F2 (moderate fibrosis: few septa), F3 (severe fibrosis: numerous septa without cirrhosis) and F4 (cirrhosis). Activity of necroinflammation was graded on a scale of 0–3: A0 (no activity), A1 (mild activity), A2 (moderate activity) and A3 (severe activity). Percentage of steatosis was quantified by determining the average proportion of hepatocytes affected by steatosis and was graded on a scale of 0–3: grade 0 (no steatosis), grade 1 (0–9%), grade 2 (10–29%), and grade 3 (over 30%). Size of steatosis was categorized into micro-vesicular, macro-vesicular and mixed types. Localization of steatosis was categorized into either centrilobular or diffuse pattern. Definition of changes in the grade of steatosis was as follows: worsening as 1 point or more increase, improvement as 1 point or more decrease, and stability as no change.

2.3. Changes in fibrosis-staging score overtime

Changes in progression of fibrosis were defined as follows: progression of fibrosis was defined as a 1 point or more increase, regression as a 1 point or more decrease and stability as no change in the METAVIR fibrosis-staging score. In addition, because the time between paired biopsies was variable, the yearly rate of progression of fibrosis was calculated as the change in fibrosis-staging score divided by the time between paired biopsies, as originally described by Poynard et al. [6].

2.4. Statistical analysis

The STAT View software package was used for statistical analysis. Categorical data were analyzed using the Fisher's exact test. Continuous variables were compared with the Student's t test. Variables that were statistically significant in univariate analysis were included in multivariate analysis using logistic regression analysis. The Kaplan–Meier method and log-rank test were used to analyze the time to occurrence of fibrosis progression. A p-value of less than 0.05 was considered statistically significant.

3. Results

3.1. Factors associated with the initial stage of fibrosis (cross-sectional study)

All three pathologists assigned the same score in 85% of patients for fibrosis staging and 95% of patients for steatosis-grading. In cases with discordance, at least two pathologists assigned the same scale. The stage of fibrosis in the initial liver biopsy was F1 in 33, F2 in 38 and F3 in 26 patients. Various clinical factors were analyzed in association with the advanced stage of fibrosis. As a result, the presence of F3 fibrosis was associated with older age, (51 ± 9 in F1–2 vs. 55 ± 9 in F3, $p = 0.03$), higher grade of histological activity (A2–3 was 35% in F1–2 vs. 84% in F3, $p = 0.0001$) and higher grade of steatosis (steatosis grade 2–3 was 34% in F1–2 vs. 58% in F3, $p = 0.04$).

The grade of steatosis was 0 in 21, 1 in 37, 2 in 25 and 3 in 14 patients. A higher grade of steatosis was associated with female gender (the male/female ratio was 35/23 in grade 0–1 vs. 15/24 in grade 2–3, $p = 0.04$), increased BMI (BMI over 25 kg/m^2 was 31% in grade 0–1 vs. 62% in grade 2–3, $p = 0.006$), and higher grade of histological activity (A2–3 was 38% in grade 0–1 vs. 62% in grade 2–3, $p = 0.03$). Multivariate logistic regression analysis revealed that increased BMI and female gender were independent factors associated with a high grade of steatosis (Table 2).

Table 2
Multivariate logistic regression analysis of factors associated with hepatic steatosis

	Odds	95% C.I.	p Value
BMI			
$\geqslant$25 kg/m^2	4.23	1.63–10.95	0.003
Gender			
Female	2.75	1.06–7.14	0.04
Activity grade			
2–3	2.30	0.85–6.26	0.10
Fibrosis stage			
3	1.63	0.53–4.97	0.39

3.2. Change in fibrosis-staging scores over time (longitudinal study)

Fibrosis staging progressed in 23% (progression by 2 points in 5% and 1 point in 18%), remained unchanged in 47% and regressed in 29% (regression by 2 points in 2% and 1 point in 27%). At first liver biopsy, laparoscopy was performed in 73 patients and the presence of cirrhosis (F4) was carefully excluded. In another 24 patients, the possibility of mis-diagnosis of F4 as F3 remains. However, the incidence of fibrosis progression did not differ according to the initial stage of fibrosis (21.2% in F1, 26.3% in F2 and 19.2% in F3, $p = 0.78$) which indicates that misdiagnosis of F4 as F3 at initial biopsy is unlikely.

Among various factors, as shown in Table 3, a higher grade of steatosis, higher levels of ALT and AST (average value for the period between the paired liver biopsies) were associated with progression of fibrosis. Since there was significant correlation between ALT and AST levels ($r = 0.684$, $p < 0.0001$), these two variables could not be analyzed together in multivariate analysis.

Table 3
Factors associated with the progression of fibrosis over time

	Progression $n = 22$	Non-progression $n = 75$	p Value
Gender: male/female	9/13	41/34	0.33
Age at biopsy: <60/$\geqslant$60 years	14/8	59/16	0.17
HCV genotype: 1b/non-1b	19/3	66/9	0.99
BMI: <25/$\geqslant$25 kg/m^2	11/11	44/31	0.48
Duration of infection (years)	32.1 ± 5.2	29.9 ± 10.0	0.56
Activity on first biopsy			
Grade: 0–1/2–3	8/14	43/32	0.10
Steatosis on first biopsy			
Grade: 0–1/2–3	6/16	52/23	0.001
Size: macro/micro/mixed	4/4/14	12/13/50	0.96
Location: centrilobular/diffuse	1/21	2/73	0.54
Evolution of steatosis			
Worsening/improvement/stable	2/2/18	9/8/58	0.09
Average ALT: <100/$\geqslant$100 IU/l	13/9	67/8	0.003
Average AST: <75/$\geqslant$75 IU/l	10/12	61/14	0.002
Interval between biopsies (years)	5.1 ± 3.2	6.2 ± 2.4	0.09
Interval between completion of IFN and second biopsy (years)	4.6 ± 3.2	5.7 ± 2.4	0.10
Treatment regimen			
RBV−/RBV+	22/0	71/4	0.27
Response to IFN			
Relapser/non-responder	16/6	53/22	0.99
Evolution of weight			
Gain/loss/stable	5/8/9	29/21/25	0.38

macro, macro-vesicular steatosis; micro, micro-vesicular steatosis; RBV−, interferon monotherapy; RBV+, interferon plus ribavirin combination therapy.
Duration of infection was determined in 38 patients whose source of infection was blood transfusion.

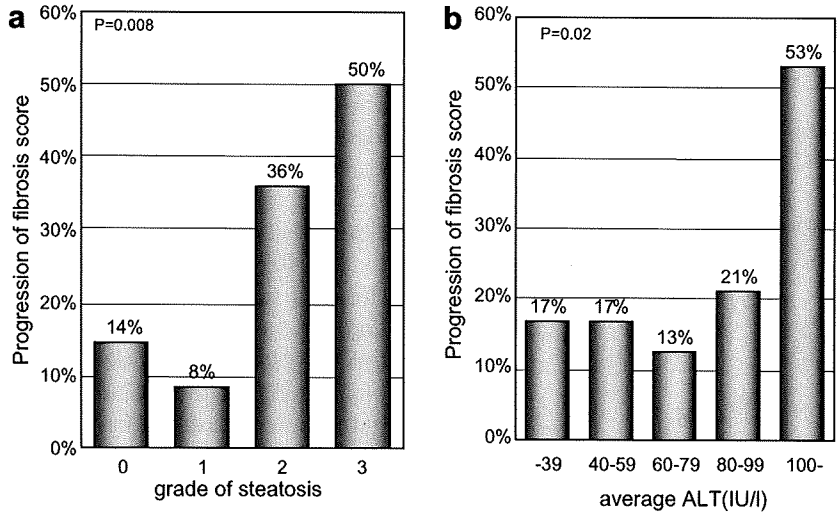

Fig. 1. Progression of fibrosis stage, hepatic steatosis and the average level of ALT. The progression of the fibrosis score over time is illustrated using bar charts. (a) Steatosis grades of 2 or 3 at initial liver biopsy were associated with the increased progression of fibrosis over time. (b) High average ALT levels during the observation period were associated with progression of fibrosis at the threshold of 100 IU/l.

Thus, average level of ALT was used for the following analysis. The probability of progression of fibrosis was 14%, 8%, 36% and 50% in patients with steatosis grades of 0, 1, 2 and 3, respectively ($p = 0.008$), and 17%, 17%, 13%, 21% and 53% in patients with average ALT values of <40, 40–59, 60–79, 80–99 and over 100 IU/l, respectively ($p = 0.02$) (Fig. 1). Multivariate logistic regression analysis revealed that these two were independent risk factors associated with the progression of fibrosis with risk ratios of 5.14 for steatosis ($p = 0.004$) and 5.21 for ALT ($p = 0.01$) (Table 4).

When patients were categorized in terms of these two risk factors, the incidence of progression of fibrosis was as high as 64% in those with both risk factors, compared to 8% in those negative for these factors. Conversely, the incidence of fibrosis regression was only 9% in those with both risk factors, compared to 37% in those negative for these factors ($p = 0.0003$) (Fig. 2).

In order to adjust for the effect of variable intervals between paired biopsies, the yearly rate of progression of fibrosis was calculated as the change in the fibrosis-staging score divided by the time between paired biopsies. The average of all patients was 0.02 ± 0.22 fibrosis units per year. Again, a higher grade of steatosis ($p = 0.004$) and higher average level of ALT ($p = 0.0005$) were associated with a higher rate of progression of fibrosis (Table 5). In addition, the yearly rate of progression of fibrosis was 0.22 ± 0.29 fibrosis units per year in those with both risk factors, 0.12 ± 0.37 in those with elevated ALT alone, 0.05 ± 0.16 in those with steatosis alone and -0.05 ± 0.17 in those negative for these two factors ($p = 0.001$). Time to progression of fibrosis at second biopsy was also analyzed by the Kaplan–Meier method. The cumulative probabilities of progression of fibrosis at five years were 58% in those with both risk factors, 33% in those with elevated ALT alone, 18% in those with steatosis alone and 2% in those negative for these two factors ($p < 0.0001$) (Fig. 3).

Table 4
Multivariate logistic regression analysis of factors associated with progression of fibrosis over time

	Odds	95% C.I.	p Value
Steatosis grade			
≥2	5.14	1.67–15.77	0.004
Average ALT			
≥100 IU/l	5.21	1.49–18.20	0.01

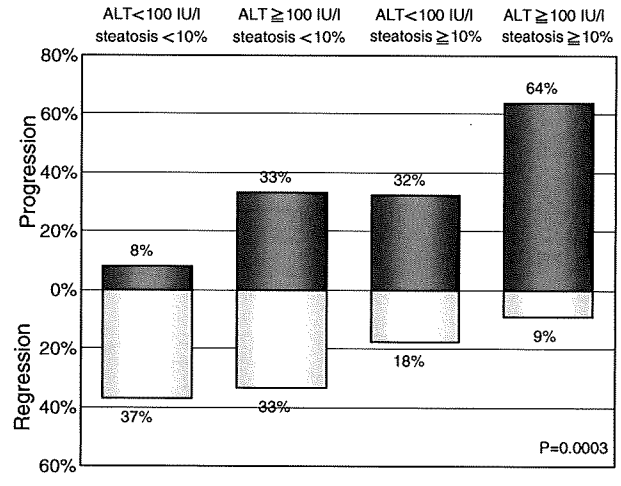

Fig. 2. Evolution of fibrosis stage in terms of risk factors. Patients were categorized into four groups according to the presence or absence of two risk factors. The upper bar chart (dark gray) indicates the progression of fibrosis while the lower bar chart (light gray) indicates the regression of fibrosis.

Table 5
Factors associated with the yearly rate of fibrosis progression

	n	Mean	SD	*p* Value
Gender				
Male	50	−0.01	0.19	0.12
Female	47	0.06	0.23	
Age at biopsy				
<60 years	73	−0.0002	0.21	0.06
⩾60 years	24	0.10	0.23	
HCV genotype				
1b	83	0.02	0.20	0.37
non-1b	14	0.08	0.32	
BMI				
<25 kg/m^2	53	0.004	0.24	0.32
⩾25 kg/m^2	44	0.05	0.19	
Steatosis on first biopsy				
0–1	58	−0.03	0.20	0.004
2–3	39	0.10	0.21	
Activity on first biopsy				
0–1	51	−0.001	0.21	0.24
2–3	46	0.05	0.22	
Fibrosis on first biopsy				
1–2	71	0.03	0.20	0.43
3	26	−0.01	0.25	
Average ALT between paired biopsies				
<100 IU/l	80	−0.01	0.17	0.0005
⩾100 IU/l	17	0.18	0.31	

4. Discussion

In the present study, we found that a higher grade of hepatic steatosis at baseline and a higher average value of ALT are independent risk factors for the progression of fibrosis over time in chronic hepatitis C patients who fail to achieve a SVR to IFN therapy. These two factors may be involved in promoting the progression of fibrosis. The association between steatosis and progression of fibrosis in untreated patients had been suggested by previous studies but this study is the first to demonstrate a similar association for treated patients. These findings are particularly important to establish a rationale for identifying therapeutic targets to halt potentially progressive disease independent of antiviral therapy.

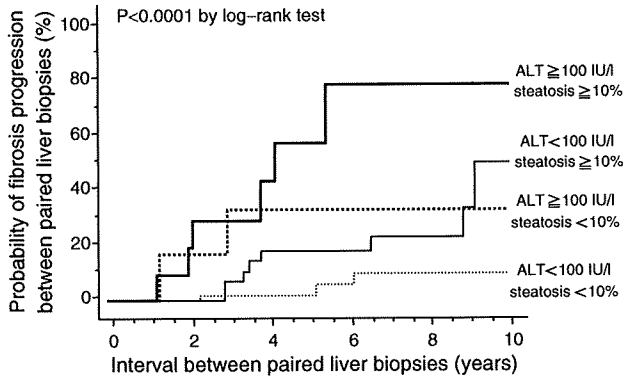

Fig. 3. Probability of fibrosis progression according to the presence of risk factors. Patients were categorized into four groups according to the presence or absence of two risk factors and the time to progression of fibrosis was analyzed.

There have been many studies that analyzed the association between steatosis and progression of liver fibrosis in HCV-infected patients, and the majority have shown a positive association [10–13], including a large scale meta-analysis [14]. However, some studies did not report this association [15–18]. There are two possible reasons for these conflicting results. First, longitudinal studies, rather than cross-sectional studies, are particularly important in the analysis of the role of steatosis in time-dependent progression of hepatic fibrosis, because cross-sectional studies involve patients with an unknown duration of steatosis. Three of four longitudinal studies that analyzed the progression of fibrosis through paired biopsies in untreated patients showed that the presence or worsening of steatosis was associated with the progression of fibrosis [12,13,20], and the probability of progression of fibrosis was significantly related to the grade of steatosis [13]. In one study, however, progression of fibrosis was correlated with older age, periportal necroinflammation and ALT elevations but not with steatosis [17]. Interestingly, steatosis was associated with older age, higher body mass index and ALT elevations in that study, indicating an indirect association of steatosis and fibrosis progression. The authors assumed that steatosis was the result rather than the cause of inflammation. This observation highlights the second reason for the controversies over a correlation between the presence of steatosis and progression of fibrosis, that is, there are so many confounding factors associated with both steatosis and fibrosis progression such as older age, advanced stage of fibrosis, higher degree of inflammation, elevated ALT, increased body mass index and insulin resistance. Because it is very difficult to prove a causal relationship between these confounding factors through clinical observations, steatosis may be a hallmark of the progression of fibrosis but it is unclear whether the effect of steatosis on progression of fibrosis is direct or mediated by other confounding factors.

Hepatic steatosis is a common pathological finding in patients with chronic hepatitis C [9]. Because the proportion of patients with steatosis is higher than would be expected from a chance association, a direct role of HCV in the pathogenesis of steatosis is suggested, at least in some patients with genotype 3 infection [21]. Furthermore, other observations suggest that steatosis may be metabolic; it is correlated with a high body mass index, visceral adiposity and insulin resistance, especially in non-3a genotypes and metabolic steatosis also is correlated with progression of fibrosis [11,22]. The

most reliable evidence that metabolic steatosis is associated with progression of fibrosis is shown by a study indicating that weight reduction in patients with chronic hepatitis C leads to a reduction in steatosis and an improvement in fibrosis, despite the persistence of HCV infection. A reduction in steatosis was significantly associated with a decrease in stellate cell activation and regression of hepatic fibrosis in 56% of patients. Thus, weight reduction may provide an important new adjunct treatment strategy for patients with chronic hepatitis C [23]. A recent study showed that the administration of pioglitazone led to metabolic and histological improvement in subjects with non-alcoholic steatohepatitis [24]. Whether amelioration of insulin resistance could improve steatosis and fibrosis in chronic hepatitis C awaits future investigation.

The mechanism by which steatosis could aggravate hepatic fibrosis in chronic hepatitis C patients remains largely hypothetical. Steatosis related insulin resistance may contribute to hyperinsulinemia and increased hepatic expression of connective tissue growth factor leading to progression of fibrosis [25]. Alternatively, a steatohepatitis-like pathway may be involved where steatosis requires a second hit for progression to fibrosis [26]. The most likely candidate is an oxidative stress with subsequent lipid peroxidation which is reported to correlate with the stage of fibrosis [27]. Another important candidate is an antiviral inflammatory response. It is reported that steatotic liver has increased susceptibility to inflammatory response [28] and that a higher grade of steatosis is correlated with a higher degree of inflammation or elevated ALT [14,15,17]. Higher degree of inflammation or elevated ALTs are associated with the progression of fibrosis [29,30], but hepatic steatosis may be responsible for the amplification of hepatic inflammation and vice versa, and the coexistence of these two factors may lead to further progression of fibrosis, as in patients with non-alcoholic steatohepatitis. In our study, average value of ALT between two biopsies was associated with fibrosis progression, whereas histological inflammation at first liver biopsy was not. The reason for this discordance may be explained by the dynamic process of hepatic necroinflammation. Severity of histological inflammation at the time of biopsy may not reflect subsequent inflammation process, whereas average value of regularly determined ALT may reflect entire fluctuation of hepatic inflammation. If so, our finding may support the hypothesis that co-operation of steatosis as the first hit and dynamic process of hepatic inflammation as the second hit promotes fibrosis progression. On the other hand, elevation of ALT may not be a mere reflection of hepatic inflammation so much as hepatocellular death such as apoptosis. Since it is reported that apoptotic caspase activation is elevated in HCV-associated steatosis [31] and that steatotic liver has increased susceptibility to apoptosis [28], elevation of ALT may also reflect an apoptosis amplified by steatosis which may lead to fibrosis progression.

Regardless of the precise mechanism, the results of the present study suggest that lowering of ALT levels may be beneficial in preventing progression of fibrosis in patients who failed to achieve a SVR. In our population, all patients received 24 weeks of IFN therapy and none received long-term maintenance therapy aiming to ameliorate hepatic inflammation. However, we speculate that amelioration of hepatic inflammation and lowering ALT levels by long-term IFN may prevent fibrosis progression in patients who remain viremic since it has been reported that IFN slowed the natural progression of fibrosis in patients who failed IFN therapy when the rate of progression of fibrosis after IFN therapy was compared to the estimated rate of progression before therapy [2,32], and that treatment duration was associated with the reduction of fibrosis independent of virological response [2]. Another possible approach to lower ALT levels may be the use of ursodeoxycholic acid, which has been reported to induce an almost 30% decrease in serum ALT levels [33,34]. The long-term efficacy of therapies targeted to the reduction of hepatic fibrosis needs future verification.

Some factors related to fibrosis progression in previous studies such as obesity [35] and worsening of steatosis [20] were not significant in our study. In our study where the majority of the population had normal body weight and very few had obesity (BMI $\geqslant 30\ kg/m^2$), impact of increased BMI on fibrosis progression may not be evaluated. Also, a smaller number of patients with worsening of steatosis (11.3% in present study and 34% in previous study [20]) may be the reason for the discrepancy. This may be due to difference in patient selection since no patients in that study had antiviral treatment between two biopsies.

In conclusion, the presence of hepatic steatosis and elevated ALT levels are risk factors for progression of fibrosis in chronic hepatitis C patients who failed to achieve a SVR to IFN therapy. These two factors may be a therapeutic target to halt the potentially progressive disease independent of antiviral therapy.

References

[1] Liang TJ, Rehermann B, Seeff LB, Hoofnagle JH. Pathogenesis, natural history, treatment, and prevention of hepatitis C. Ann Intern Med 2000;132:296–305.

[2] Poynard T, McHutchison J, Davis GL, Esteban-Mur R, Goodman Z, Bedossa P, et al. Impact of interferon alfa-2b and ribavirin on progression of liver fibrosis in patients with chronic hepatitis C. Hepatology 2000;32:1131–1137.

[3] Yoshida H, Shiratori Y, Moriyama M, Arakawa Y, Ide T, Sata M, et al. Interferon therapy reduces the risk for hepatocellular carcinoma: national surveillance program of cirrhotic and noncirrhotic patients with chronic hepatitis C in Japan. IHIT Study Group. Inhibition of Hepatocarcinogenesis by Interferon Therapy. Ann Intern Med 1999;131:174–181.

[4] Manns MP, McHutchison JG, Gordon SC, Rustgi VK, Shiffman M, Reindollar R, et al. Peginterferon alfa-2b plus ribavirin compared with interferon alfa-2b plus ribavirin for initial treatment of chronic hepatitis C: a randomised trial. Lancet 2001;358:958–965.
[5] Fried MW, Shiffman ML, Reddy KR, Smith C, Marinos G, Goncales Jr FL, et al. Peginterferon alfa-2a plus ribavirin for chronic hepatitis C virus infection. N Engl J Med 2002;347:975–982.
[6] Poynard T, Bedossa P, Opolon P. Natural history of liver fibrosis progression in patients with chronic hepatitis C. The OBSVIRC, METAVIR, CLINIVIR, and DOSVIRC groups. Lancet 1997;349:825–832.
[7] Marcellin P, Asselah T, Boyer N. Fibrosis and disease progression in hepatitis C. Hepatology 2002;36:S47–S56.
[8] Alberti A, Vario A, Ferrari A, Pistis R. Review article: chronic hepatitis C – natural history and cofactors. Aliment Pharmacol Ther 2005;22 Suppl 2:74–78.
[9] Lefkowitch JH, Schiff ER, Davis GL, Perrillo RP, Lindsay K, Bodenheimer Jr HC, et al. Pathological diagnosis of chronic hepatitis C: a multicenter comparative study with chronic hepatitis B. The Hepatitis Interventional Therapy Group. Gastroenterology 1993;104:595–603.
[10] Hourigan LF, Macdonald GA, Purdie D, Whitehall VH, Shorthouse C, Clouston A, et al. Fibrosis in chronic hepatitis C correlates significantly with body mass index and steatosis. Hepatology 1999;29:1215–1219.
[11] Adinolfi LE, Gambardella M, Andreana A, Tripodi MF, Utili R, Ruggiero G. Steatosis accelerates the progression of liver damage of chronic hepatitis C patients and correlates with specific HCV genotype and visceral obesity. Hepatology 2001;33:1358–1364.
[12] Westin J, Nordlinder H, Lagging M, Norkrans G, Wejstal R. Steatosis accelerates fibrosis development over time in hepatitis C virus genotype 3 infected patients. J Hepatol 2002;37:837–842.
[13] Fartoux L, Chazouilleres O, Wendum D, Poupon R, Serfaty L. Impact of steatosis on progression of fibrosis in patients with mild hepatitis C. Hepatology 2005;41:82–87.
[14] Leandro G, Mangia A, Hui J, Fabris P, Rubbia-Brandt L, Colloredo G, et al. Relationship between steatosis, inflammation, and fibrosis in chronic hepatitis C: a meta-analysis of individual patient data. Gastroenterology 2006;130:1636–1642.
[15] Asselah T, Boyer N, Guimont MC, Cazals-Hatem D, Tubach F, Nahon K, et al. Liver fibrosis is not associated with steatosis but with necroinflammation in French patients with chronic hepatitis C. Gut 2003;52:1638–1643.
[16] Hui JM, Sud A, Farrell GC, Bandara P, Byth K, Kench JG, et al. Insulin resistance is associated with chronic hepatitis C virus infection and fibrosis progression [corrected]. Gastroenterology 2003;125:1695–1704.
[17] Perumalswami P, Kleiner DE, Lutchman G, Heller T, Borg B, Park Y, et al. Steatosis and progression of fibrosis in untreated patients with chronic hepatitis C infection. Hepatology 2006;43:780–787.
[18] Conjeevaram HS, Kleiner DE, Everhart JE, Hoofnagle JH, Zacks S, Afdhal NH, et al. Race, insulin resistance and hepatic steatosis in chronic hepatitis C. Hepatology 2007;45:80–87.
[19] Bedossa P, Poynard T. An algorithm for the grading of activity in chronic hepatitis C. The METAVIR Cooperative Study Group. Hepatology 1996;24:289–293.
[20] Castera L, Hezode C, Roudot-Thoraval F, Bastie A, Zafrani ES, Pawlotsky JM, et al. Worsening of steatosis is an independent factor of fibrosis progression in untreated patients with chronic hepatitis C and paired liver biopsies. Gut 2003;52:288–292.
[21] Mihm S, Fayyazi A, Hartmann H, Ramadori G. Analysis of histopathological manifestations of chronic hepatitis C virus infection with respect to virus genotype. Hepatology 1997;25:735–739.
[22] Fartoux L, Poujol-Robert A, Guechot J, Wendum D, Poupon R, Serfaty L. Insulin resistance is a cause of steatosis and fibrosis progression in chronic hepatitis C. Gut 2005;54:1003–1008.
[23] Hickman IJ, Clouston AD, Macdonald GA, Purdie DM, Prins JB, Ash S, et al. Effect of weight reduction on liver histology and biochemistry in patients with chronic hepatitis C. Gut 2002;51:89–94.
[24] Belfort R, Harrison SA, Brown K, Darland C, Finch J, Hardies J, et al. A placebo-controlled trial of pioglitazone in subjects with nonalcoholic steatohepatitis. N Engl J Med 2006;355:2297–2307.
[25] Paradis V, Perlemuter G, Bonvoust F, Dargere D, Parfait B, Vidaud M, et al. High glucose and hyperinsulinemia stimulate connective tissue growth factor expression: a potential mechanism involved in progression to fibrosis in nonalcoholic steatohepatitis. Hepatology 2001;34:738–744.
[26] Day CP, James OF. Steatohepatitis: a tale of two "hits"? Gastroenterology 1998;114:842–845.
[27] Paradis V, Mathurin P, Kollinger M, Imbert-Bismut F, Charlotte F, Piton A, et al. In situ detection of lipid peroxidation in chronic hepatitis C: correlation with pathological features. J Clin Pathol 1997;50:401–406.
[28] Walsh MJ, Vanags DM, Clouston AD, Richardson MM, Purdie DM, Jonsson JR, et al. Steatosis and liver cell apoptosis in chronic hepatitis C: a mechanism for increased liver injury. Hepatology 2004;39:1230–1238.
[29] Mathurin P, Moussalli J, Cadranel JF, Thibault V, Charlotte F, Dumouchel P, et al. Slow progression rate of fibrosis in hepatitis C virus patients with persistently normal alanine transaminase activity. Hepatology 1998;27:868–872.
[30] Ghany MG, Kleiner DE, Alter H, Doo E, Khokar F, Promrat K, et al. Progression of fibrosis in chronic hepatitis C. Gastroenterology 2003;124:97–104.
[31] Seidel N, Volkmann X, Langer F, Flemming P, Manns MP, Schulze-Osthoff K, et al. The extent of liver steatosis in chronic hepatitis C virus infection is mirrored by caspase activity in serum. Hepatology 2005;42:113–120.
[32] Shiffman ML, Hofmann CM, Contos MJ, Luketic VA, Sanyal AJ, Sterling RK, et al. A randomized, controlled trial of maintenance interferon therapy for patients with chronic hepatitis C virus and persistent viremia. Gastroenterology 1999;117:1164–1172.
[33] Omata M, Yoshida H, Toyota J, Tomita E, Nishiguchi S, Hayashi N, et al. A large-scale, multicentre, double-blind trial of ursodeoxycholic acid in patients with chronic hepatitis C. Gut 2007;56:1747–1753.
[34] Takano S, Ito Y, Yokosuka O, Ohto M, Uchiumi K, Hirota K, et al. A multicenter randomized controlled dose study of ursodeoxycholic acid for chronic hepatitis C. Hepatology 1994;20:558–564.
[35] Ortiz V, Berenguer M, Rayon JM, Carrasco D, Berenguer J. Contribution of obesity to hepatitis C-related fibrosis progression. Am J Gastroenterol 2002;97:2408–2414.

Hepatology Research 2008; 38: 909–918 doi: 10.1111/j.1872-034X.2008.00352.x

Original Article

Griseofulvin, an oral antifungal agent, suppresses hepatitis C virus replication *in vitro*

Haofan Jin,[1] Atsuya Yamashita,[1] Shinya Maekawa,[2] Pinting Yang,[1,3] Limin He,[1] Satoru Takayanagi,[1] Takaji Wakita,[4] Naoya Sakamoto,[5] Nobuyuki Enomoto[2] and Masahiko Ito[1]

[1]*Department of Microbiology,* [2]*First Department of Internal Medicine, University of Yamanashi, Yamanashi, and* [5]*Department of Gastroenterology and Hepatology, Tokyo Medical and Dental University, Tokyo, Japan;* [3]*Department of Rheumatology and Immunology, China Medical University, Shenyang, China; and* [4]*Department of Virology II, National Institute of Infectious Diseases, Tokyo, Japan*

Aim: Hepatitis C virus (HCV), which infects an estimated 170 million people worldwide, is a major cause of chronic liver disease. The current standard therapy for chronic hepatitis C is based on pegylated interferon (IFN)α in combination with ribavirin. However, the success rate remains at approximately 50%. Therefore, alternative agents are needed for the treatment of HCV infection.

Methods: Using an HCV-1b subgenomic replicon cell culture system (Huh7/Rep-Feo), we found that griseofulvin, an oral antifungal agent, suppressed HCV-RNA replication and protein expression in a dose-dependent manner. We also found that griseofulvin suppressed the replication of infectious HCV JFH-1. A combination of IFNα and griseofulvin exhibited a synergistic inhibitory effect in Huh7/Rep-Feo cells.

Results: We found that griseofulvin blocked the cell cycle at the G_2/M phase in the HCV subgenomic replicon cells, but did not inhibit HCV internal ribosome entry site-dependent translation.

Conclusion: Our results suggest that griseofulvin may represent a new approach to the development of a novel therapy for HCV infection.

Key words: cell cycle, griseofulvin, hepatitis C virus internal ribosome entry site, hepatitis C virus replicon, JFH-1

INTRODUCTION

HEPATITIS C VIRUS (HCV) is an etiologic agent of chronic liver disease,[1,2] and it is estimated that approximately 170 million people worldwide are infected with the virus. Chronic hepatitis C can lead to severe liver diseases, including fibrosis, cirrhosis, and hepatocellular carcinoma.[3] With advancements in HCV therapy, including the most recent combination of pegylated interferon (IFN)α and ribavirin, up to one-half of patients achieve a sustained virological response. However, the remainder cannot clear the virus, demonstrating a great need for more powerful therapeutic modalities.[4]

Investigations have been hampered by the lack of an efficient HCV cell culture system. In 1999, the establishment of an HCV subgenomic replicon cell culture system improved the situation. The subgenomic replicon RNA is composed of the HCV 5′ untranslated region (UTR) containing the internal ribosomal entry site (IRES), a neomycin phosphotransferase (neo) gene and the HCV non-structural (NS) proteins through 3–5B under the control of an encephalomyocarditis virus (EMCV) IRES, followed by the HCV 3′ UTR.[5] A HCV replicon carrying, in addition to the selectable marker, a gene encoding luciferase, can be used to screen a large number of compounds for antiviral activity.[6–8] The recent development of an *in vitro* HCV infection system provides an opportunity to evaluate inhibitors of all stages of the HCV life cycle.[9–11]

Correspondence: Dr Atsuya Yamashita, Department of Microbiology, Division of Medicine, Interdisciplinary Graduate School of Medicine and Engineering, University of Yamanashi,, 1110 Shimokato, Chuo, Yamanashi 409-3898, Japan. Email: atsuyay@yamanashi.ac.jp
Received 12 September 2007; revision 31 January 2008; accepted 11 February 2008.

Currently, proof of concept has been obtained in clinical trials of three different HCV NS3 protease inhibitors, BILN 2061,[12,13] telaprevir (VX-950),[14] and SCH 503034.[15] However, because of many factors, including possible side-effects and the emergence of drug-resistant mutants, there is still great need for improved therapies. We focused therefore on screening a set of licensed drugs which have not been recommended previously for antiviral use. Here, we found that the oral antifungal agent, griseofulvin, had a suppressive effect on HCV replication, assessed using the HCV-1b subgenomic replicon system and the particle-producing cell culture HCV-2a model of JFH-1. The mechanism of the anti-HCV activity of griseofulvin also was studied.

METHODS

Cell cultures and HCV replicon

THE HUMAN HEPATOMA cell line, Huh7, was maintained in Dulbecco's modified Eagle's medium (DMEM) supplemented with 10% (v/v) fetal bovine serum, 100 IU/mL penicillin, and 100 μg/mL streptomycin. For subgenomic replicon Huh7/Rep-Feo (HCV 1b replicon that expresses a chimeric protein consisting of neomycin phosphotransferase and firefly luciferase) cells,[7,8] the culture medium was supplemented with 250 g/mL G418. Huh 7.5.1/JFH-1 cells (Huh 7.5.1 chronically infected HCV JFH-1) were maintained in DMEM supplemented with 10% (v/v) fetal bovine serum, 100 IU/mL penicillin, and 100 μg/mL streptomycin.[16]

Reagents

Griseofulvin and fluconazole were purchased from Wako Pure Chemical (Tokyo, Japan). Itraconazole was purchased from LKT Laboratories (St Paul, MN, USA). Recombinant human IFNα-2b was purchased from Santa Cruz Biotechnology (Santa Cruz, CA, USA).

Cell viability assays

For griseofulvin and fluconazole, viable cell growth was determined by a 5-(3-carboxymethoxyphenyl)-2-(4,5-dimethylthiazoly)-3-(4-sulfophenyl) tetrazolium inner salt (MTS) reduction assay using the Cell Titer 96 aqueous one solution cell proliferation assay (Promega, Madison, WI, USA), according to the manufacturer's protocol.

For itraconazole, viable cell growth was determined using the CellTiter-Glo luminescent cell viability assay (Promega, USA), according to the manufacturer's protocol.

Luciferase activity assays

Typically, Huh7/Rep-Feo cells were seeded in a 48-well plate at a density of 2×10^4 cells per well. Compounds were added to the culture medium at various concentrations. After 72 h of culture, the expression levels of the HCV replicon were measured by luciferase assay using the luciferase assay system (Promega, USA) and the Luminescencer-JNR AB-2100 (Atto, Tokyo, Japan).

The Huh7 cells stably transfected with the pEF Fluc IN vector were mock treated (control) or treated with 20 μM or 40 μM griseofulvin. After 72 h of culture, luciferase assays were performed using the luciferase assay system and the Luminescencer-JNR AB-2100. Luciferase activity was normalized by the protein concentration, measured using a BCA protein assay kit (Pierce, Rockford, IL, USA).

The Huh7 cells stably transfected with the pEF Rluc-HCV IRES Feo vector were mock treated (control) or treated with 20 μM griseofulvin. Dual luciferase activities were carried out at 8, 16, 24, and 32 h after exposure to griseofulvin using the dual luciferase reporter assay system and the Luminescencer-JNR AB-2100.

All assays were performed in triplicate, and the results were expressed as mean ± SD relative light units.

RNA analysis

Total cellular RNA was extracted from the Huh7/Rep-Feo cells using the RNAqueous-4PCR kit (Ambion, Austin, TX, USA). RNA was reverse transcribed with a Thermoscript reverse transcriptase kit (Invitrogen, Carlsbad, CA, USA).

Quantitative real-time polymerase chain reaction (PCR) was carried out using ABI Prism 7500 (Applied Biosystems, Foster City, CA, USA). The forward and reverse primers for the 5′ UTR of HCV-RNA were 5′-TGCGGAACCGGTGAGTACA-3′ and 5′-CTTAAGG TTTAGGATTCGTGCTCAT-3′, respectively. The fluorogenic probe used for the quantification of HCV-RNA was 5′-(FAM)-CACCCTATCAGGCAGTA-CCACAAGG CC-(TAMRA)-3′. Human 18S ribosomal RNA levels in the samples were analyzed by quantitative real-time PCR to normalize the RNA content. The forward and reverse primers for human 18S ribosomal RNA were 5′-ACTCTAGATAACCTCGGGCCGA-3′ and 5′-GATGT GGTAGCCGTTTCTCAGG-3′, respectively. The fluorogenic probe used for quantification of human 18S ribo-

somal RNA was 5′-(FAM)-CCATTCGAACGTCTGCCC TATCAACTTT-(TAMRA)-3′. The method has been described elsewhere.[17]

The primers used for reverse transcription (RT)–PCR were as follows: human 2′,5′-oligoadenylate synthetase (2′,5′-OAS): forward primer, 5′-CAATCAGCGAGGCC AGTAATC-3′ and reverse primer, 5′-TGGTGAGAAGTGC TGGGGTC-3′; human myxovirus resistance protein A (MxA): forward primer, 5′-GTCAGGAGT-TGCCCTT CCCA-3′ and reverse primer, 5′-GGCCCCTTCCTT ACCCTTA-3′; and human glyceraldehyde-3-phosphate dehydrogenase (GAPDH): forward primer, 5′-GAAG GTGAAGGTCGGAGTC-3′ and reverse primer, 5′-CTT TAGGGTAGTGGTAGAAG-3′, respectively. Each reaction mixture contained cDNA (3 μL), 1.5 mM $MgCl_2$, 200 μM dNTP, 1 μM each primer, and 1.25 U AmpliTaq Gold (Applied Biosystems, USA) with 1× supplied reaction buffer. After activation of AmpliTaq Gold activity at 95 °C for 10 min, the temperature cycling conditions for MxA were 29 cycles consisting of denaturation at 95 °C for 30 s, annealing at 56 °C for 1 min, and extension at 72 °C for 1 min. For 2′,5′-OAS, the conditions were 32 cycles consisting of denaturation at 95 °C for 30 s, annealing at 53 °C for 1 min, and extension at 72 °C for 1 min. For GAPDH, the conditions were 30 cycles consisting of denaturation at 95 °C for 30 s, annealing at 53 °C for 1 min, and extension at 72 °C for 1 min. PCR products were subjected to electrophoresis in a 3% agarose gel.

Western blotting

Preparation of cell lysates, sodium dodecyl sulfate–polyacrylamide gel electrophoresis, and immunoblotting were performed as described previously.[18] The antibodies used in this study were the anti-NS3 antibody (Santa Cruz Biotechnology, USA) anti-NS5A antibody (Virogen, Watertown, MA, USA) and anti-β-actin antibody (Cell Signaling, Danvers, MA, USA). Alkaline phosphatase-conjugated secondary antibodies and CDP-Star chemiluminescent substrate (New England Biolabs, Beverly, MA, USA) were used for detection.

Cell cycle analysis

Harvested cells were washed once with phosphate-buffered saline (PBS) and fixed with 70% ethanol at 4 °C for 1 h. After an additional wash, the cells were treated with 250 μg/mL RNase A at 37 °C for 1 h and subsequently stained with 50 μg/mL propidium iodide at 4 °C for 1 h. The DNA content was then analyzed by FACSCalibur (BD Biosciences, Franklin Lakes, NJ, USA) with ModFit LT software (Verity Software House, Topsham, ME, USA).

Analyses of drug synergy

The effects of the treatment of Huh7/Rep-Feo cells with griseofulvin and IFNα, alone and in combination, were analyzed with CalcuSyn, a computer program based on the method of Chou and Talalaly.[19] After converting the dose-effect curves for each drug or drug combination to median-effect plots, the program calculated a combination index (CI). The CI of <1, 1, and >1 indicate synergy, an additive effect, and antagonism, respectively.

Plasmids and stable transfection

The plasmid pEF-Fluc-IN was constructed as follows. The fragment carrying the firefly luciferase was amplified from the pGL3 control vector (Promega, USA) by PCR using a pair of primers (5′-GAATTCATGGAAGAC GCCAAAAACATAAA-3′ [*Eco*RI site] and 5′-GCGGC CGCTTACACGGCGATCTTTCCGCCC-3′ [*Not*I site]). The PCR product was cloned into the pGEM-T Easy vector (Promega, USA). The EMCV IRES Neo fragment was excised from the pMXs-IN vector by *Not*I and *Sal*I digestion.[20] The *Eco*RI–*Sal*I fragment of the pCHO vector was excised from the pGag-pol-IRES-bs^r vector by *Eco*RI and *Sal*I digestion.[21] To construct pEF-Fluc-IB, the *Eco*RI–*Not*I fragment of firefly luciferase, and the *Not*I–*Sal*I fragment of the EMCV IRES Neo were inserted into the *Eco*RI and the *Sal*I site of pCHO by triple ligation.

The plasmid pEF Rluc-HCV IRES Feo was constructed as follows. The fragment carrying the Renilla luciferase was amplified from the phRL-TK vector (Promega, USA) by PCR using a pair of primers (5′-GAATTCATGGCT TCCAAGGTGTACGACCC-3′ [*Eco*RI site] and 5′-GGAT CCTTACTGCTCGTTCTTCAGCACGC-3′ [*Bam*HI site]). The fragment carrying the HCV IRES Feo was amplified from the pRep-Feo vector[7] by PCR using a pair of primers (5′-GGATCCGCCAGCCCCCGATTGGGGGCG AC-3′ [*Bam*HI site] and 5′-GTCGACTCAGAAGAAC TCGTCAAGAAGGC-3′ [*Sal*I site]). Each PCR product was cloned into the pGEM-T Easy vector. To construct pEF Rluc-HCV IRES Feo, the *Eco*RI–*Bam*HI fragment of Renilla luciferase, and the *Bam*HI–*Sal*I fragment of HCV IRES Feo were inserted into the *Eco*RI and *Sal*I site of pCHO by triple ligation.

The pEF-Fluc-IB and pEF Rluc-HCV IRES Feo was transfected into Huh7 cells using Effectene transfection reagent (QIAGEN, Hilden, Germany), according to the manufacturer's recommendation. Two days after trans-

fection, the Huh7 cells were selected in a medium containing 250 μg/mL G418.

Immunofluorescent staining

After treatment with griseofulvin for 72 h, HCV JFH-1-infected cells were fixed with cold methanol and blocked using Blocking One (Nacalai Tesque, Kyoto, Japan). For the detection of the NS3 protein, the cells were incubated with the anti-NS3 antibody (Virogen, USA) for 1 h at room temperature. After washing with PBS, the cells were incubated with an Alexa Fluor 488 goat antimouse immunoglobulin G antibody (Molecular Probes, Eugene, OR, USA) for 1 h at room temperature. After washing with PBS, the cells were stained with 7-aminoactinomycin D for nuclear counterstaining, and analyzed using fluorescence microscopy.

RESULTS

Replication of a subgenomic HCV-1b replicon is suppressed by griseofulvin

WE INVESTIGATED THE anti-HCV effect and cell toxicity of griseofulvin in the HCV subgenomic replicon cells, Huh7/Rep-Feo. The luciferase activities of the Huh7/Rep-Feo cells showed that replication of the HCV replicon was suppressed by griseofulvin in a dose-dependent manner (Fig. 1a). Next, we performed a time-course experiment in which the luciferase activities of Huh7/Rep-Feo cells were measured at various time points after treatment with griseofulvin. As shown in Figure 1b, griseofulvin induced a decrease in the luciferase activities of Huh7/Rep-Feo cells over time. The treatment with griseofulvin had little effect on cellular viability at this range of concentration, as revealed by the MTS assay (Fig. 1c). The 50% effective concentration (EC_{50}) of griseofulvin was 6.13 ± 0.17 μM. The 50% cytotoxic concentration of this compound (CC_{50}) was 217.93 ± 3.49 μM. Thus the selectivity index (ratio of CC_{50} to EC_{50}) was 35.5 (Table 1). Furthermore, we examined the effect of other antifungal agents, fluconazole and itraconazole, on HCV-RNA replication. In contrast, fluconazole and itraconazole had little effect on HCV-RNA replication (Table 1).

We analyzed HCV-RNA levels in Huh7/Rep-Feo cells treated or not treated with griseofulvin using real-time RT–PCR. As shown in Figure 2a, treatment with griseofulvin decreased the replicon RNA titer in a dose-dependent manner. Similar results were seen at the protein level by monitoring the HCV non-structural proteins NS3 and NS5A. The Western blot analysis demon-

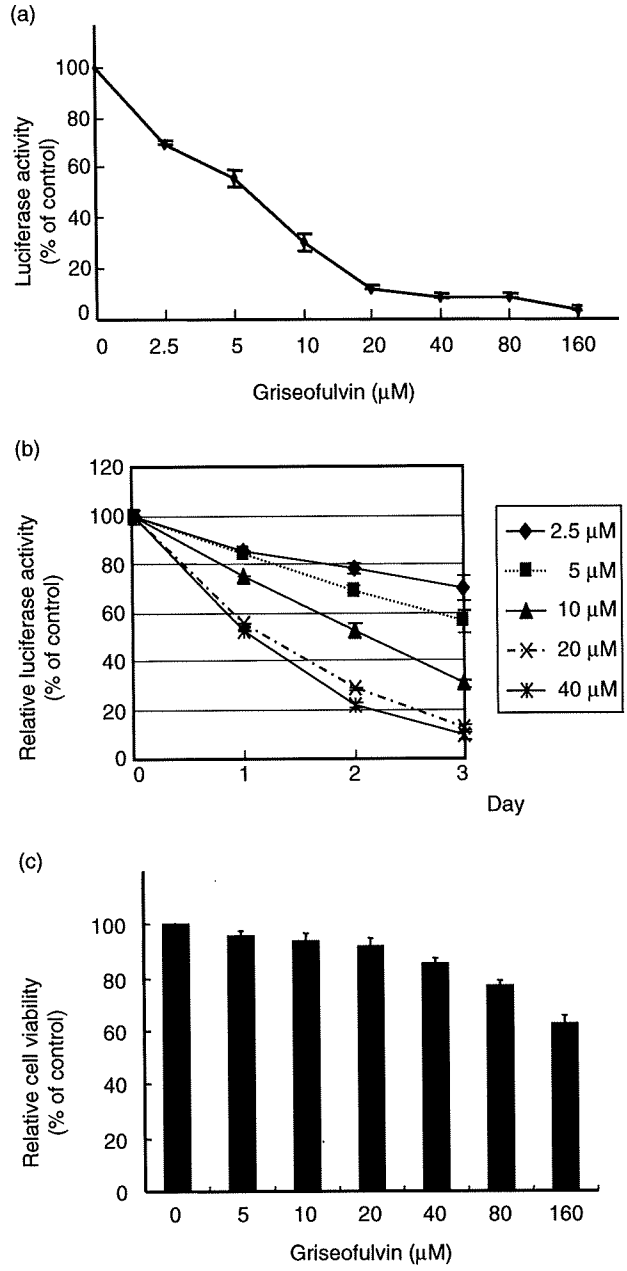

Figure 1 Inhibition of hepatitis C virus replication in Huh7/Rep-Feo cells by griseofulvin. (a) Huh7/Rep-Feo cells were cultured with various concentrations of griseofulvin in the medium and luciferase assays were performed after 72 h of culture. Luciferase assays were performed in triplicate. Error bars indicate mean ± standard deviation. (b) Huh7/Rep-Feo cells were treated with various concentrations of griseofulvin (2.5–40.0 μM). Luciferase activity was measured at the time points indicated after exposure to griseofulvin. (C) 5-(3-Carboxymethoxyphenyl)-2-(4,5-dimethylthiazoly)-3-(4-sulfophenyl) tetrazolium inner salt of Huh7/Rep-Feo cells cultured with the concentration of griseofulvin indicated.

Table 1 Antihepatitis C virus activities of oral antifungal agents in Huh7/Rep-Feo cells†

	EC_{50} (μM)	CC_{50} (μM)	SI
Griseofulvin	6.13 ± 0.17	217.93 ± 3.49	35.5
Fluconazole	135.6 ± 1.25	159.06 ± 1.07	1.2
Itraconazole	1.24 ± 0.21	3.35 ± 0.17	2.7

†All data represent means ± standard deviation for three separate experiments. CC_{50}, 50% cytotoxicity concentration based on the reduction of cell viability; EC_{50}, 50% effective concentration based on the inhibition of HCV replication; SI, selectivity index (CC_{50}/EC_{50}).

strated that griseofulvin treatment results in reduced levels of these viral proteins (Fig. 2b).

However, it remains to be clarified whether the griseofulvin inhibits firefly luciferase directly. To investigate this possibility, we examined the effect of griseofulvin on firefly luciferase activity using Huh7 cells expressing firefly luciferase constitutively. The treatment of these cells with griseofulvin resulted in no significant change in the firefly luciferase activity (Fig. 3). This result excludes the possibility that griseofulvin inhibits firefly luciferase activity directly.

Anti-HCV activity of griseofulvin is not mediated by the IFN signaling pathway

It has been reported that the HCV replicon is highly sensitive to IFN.[22,23] To determine whether the action of griseofulvin on the HCV subgenomic replicon involves the activation of IFN-stimulated gene responses, we analyzed the expression of IFN inducible genes in HCV replicon cells. The RT–PCR analysis showed that the messenger RNA for MxA and 2′,5′-OAS, which are both IFN inducible genes, were induced by IFNα-2b, but not by griseofulvin (Fig. 4). These results suggest that the action of griseofulvin on the intracellular replication of HCV replicon is independent of the IFN signaling pathway.

Synergistic inhibitory effect of griseofulvin and IFNα on HCV replicon

Whether a combination of griseofulvin and IFNα exhibits a synergistic, additive, or antagonistic effect was assessed using an isobologram method.[19] An isobologram analysis is an approach used in preclinical studies to quantify the extent of synergistic, additive, or antagonistic effects between drugs used in combination. For instance, a representation of an isobologram to evaluate a drug–drug interaction is shown in Figure 5a. It is understood that synergy, additivity, and antagonism are represented by concave, liner, and convex isoeffective curves (isoboles), respectively. The combined anti-HCV effects of griseofulvin and IFNα were evaluated. Prior to the combination experiments, the optimal concentration ratio of two compounds (combination ratio) had to be determined. After preliminary experiments, three different rations were chosen for each combination

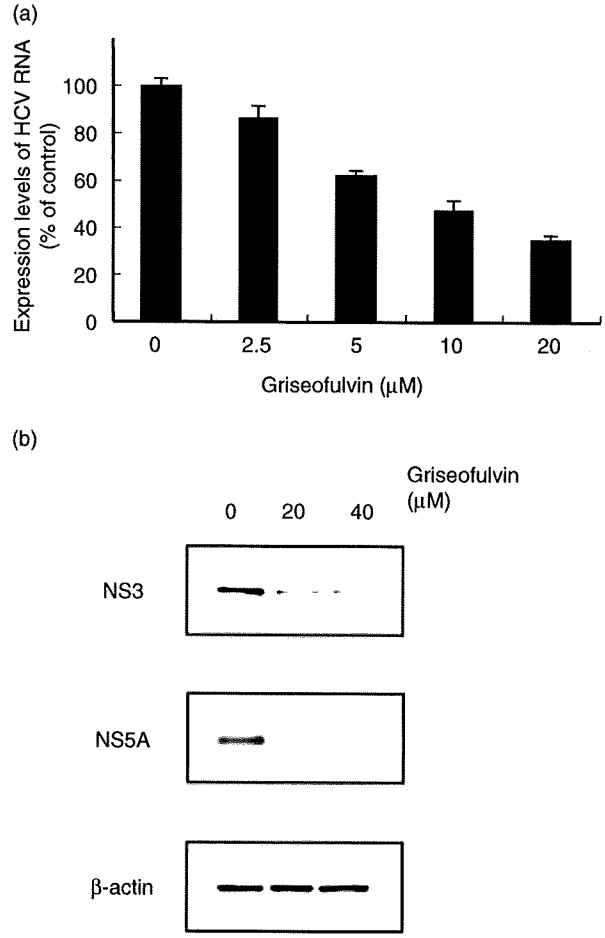

Figure 2 Suppressive effect of griseofulvin for hepatitis C virus (HCV) replicon was confirmed by real-time reverse transcription–polymerase chain reaction (RT–PCR) and Western blot analysis. (a) Incubation of Huh7/Rep-Feo cells with griseofulvin for 72 h resulted in dose-dependent antiviral effects. Real-time RT–PCR was performed on the extracted RNA. HCV-RNA levels are shown as relative percentages of untreated control. Error bars indicate mean ± SD. (b) Western blot analyses of NS3 and NS5A protein expressions were performed on protein extracts from cells that were treated for 72 h with varying dose of griseofulvin. β-Actin was used as a loading control.

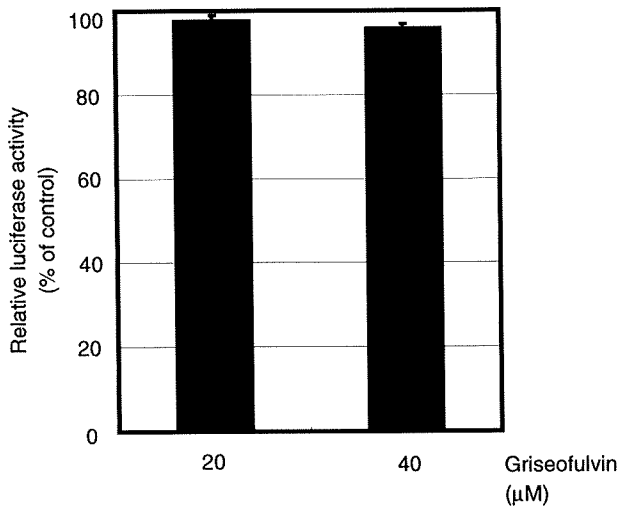

Figure 3 No inhibition of firefly luciferase activity by griseofulvin. pEF Fluc IN vector was stably transfected into Huh7 cells. Cells were cultured without (control) and with 20 μM or 40 μM griseofulvin for 72 h. Firefly luciferase assay was performed. Luciferase activity was normalized by the protein concentration. Error bars indicate mean ± SD.

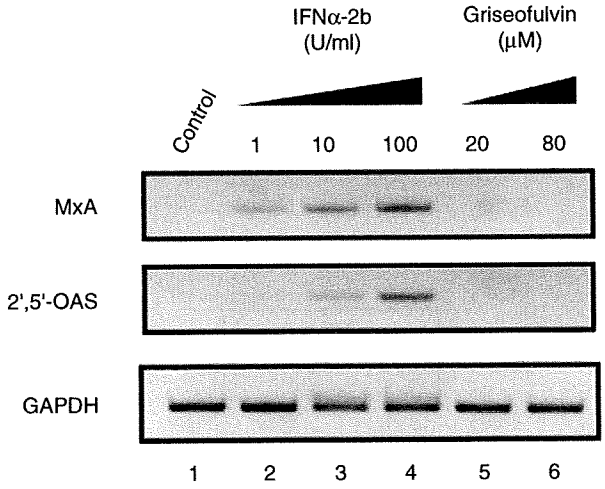

Figure 4 Griseofulvin elicited an interferon (IFN) response. Huh7/Rep-Feo cells were treated without (lane 1) or with 1, 10, or 100 U/mL IFNα-2b (lanes 2–4), and 20 (lane 5) or 80 μM griseofulvin (lane 6) for 72 h. Messenger RNA of human myxovirus resistance protein A (MxA), 2′,5′-oligoadenylate synthetase (2′,5′-OAS), and glyceraldehyde-3-phosphate dehydrogenase (GAPDH) as an internal control were detected by reverse transcription–polymerase chain reaction analysis.

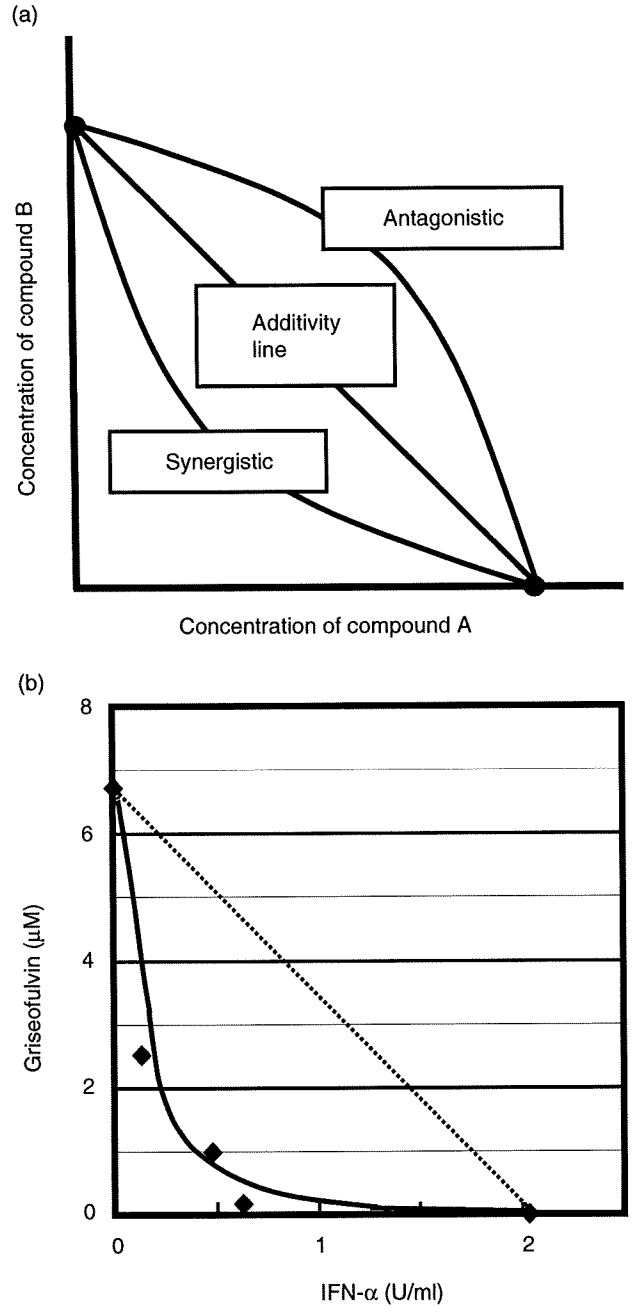

Figure 5 Effect of a combination of griseofulvin and interferon (IFN)α on intracellular hepatitis C virus (HCV)-RNA replication. (a) Representative isobologram for analyzing the interaction between two drugs. (b) Isobole plot of 50% inhibition of HCV-RNA replication. Huh7/Rep-Feo cells were treated with griseofulvin in combination with IFNα, and a luciferase assay was performed after 72 h of culture to obtain each isobole plot. Dotted line indicates an additive effect in the isobologram method used.

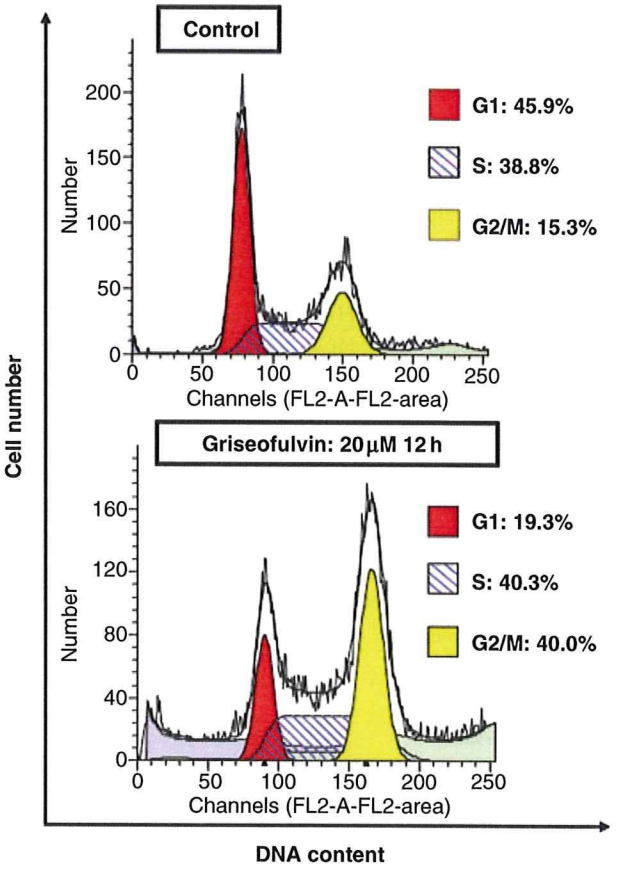

Figure 6 Griseofulvin induced G_2/M phase arrest in Huh7/Rep-Feo cells. Flow cytometry analysis of DNA content of untreated Huh7/Rep-Feo cells (control) and cells treated for 12 h with 20 μM of griseofulvin. [■ G_1: 45.9%, ▨ S: 38.8%, □ G_2/M: 15.3%; ■ G_1: 19.3%, ▨ S: 40.3%, □ G_2/M: 40.0%.]

(data not shown). The ratios of griseofulvin and IFNα were 9:1, 1:1, and 1:9. Each concentration of griseofulvin and IFNα at 50% inhibition was plotted on the X- and Y-axes, respectively, to generate an isobologram (Fig. 5b). As shown in Figure 5b, each plot fell far below the line showing additivity, indicating that the effect of the griseofulvin and IFNα combination on HCV-RNA replication is strongly synergistic.

Griseofulvin induces G_2/M cell cycle arrest in HCV replicon cells

As described previously, griseofulvin blocks cell cycle progression at the G_2/M phase in several human cell lines.[24] Here, we examined the effect of griseofulvin on cell cycle progression in Huh7/Rep-Feo cells. As shown in Figure 6, the population of griseofulvin-treated Huh7/Rep-Feo cells in the G_2/M phase at 12 h was 40%, compared to 15.3% for the control cell populations. These data imply that griseofulvin might have the potential to arrest Huh7/Rep-Feo cells in the G_2/M phase.

As described earlier, the treatment of Huh7/Rep-Feo cells with 20 μM griseofulvin for 12 h results in G_2/M arrest (Fig. 6), while treatment for 72 h had no effect on cell growth (Fig. 1c). To explain this discrepancy, we examined the growth kinetics of griseofulvin-treated Huh7/Rep-Feo cells. The cells were cultured with 20 μM griseofulvin, and cell growth was monitored by MTS assay. The cell viability declined gradually until 48 h after treatment with 20 μM griseofulvin, but increased from 48 h to 72 h (Fig. 7). These data indicate that treatment with 20 μM griseofulvin arrests Huh7/Rep-Feo cells in the G_2/M phase, but does not inhibit cell growth completely.

Griseofulvin does not inhibit HCV IRES-dependent translation

Previous studies have shown that vinblastine sulfate and nocodazole, well-characterized inhibitors of microtubule polymerization and the cell cycle in G_2/M, inhibit

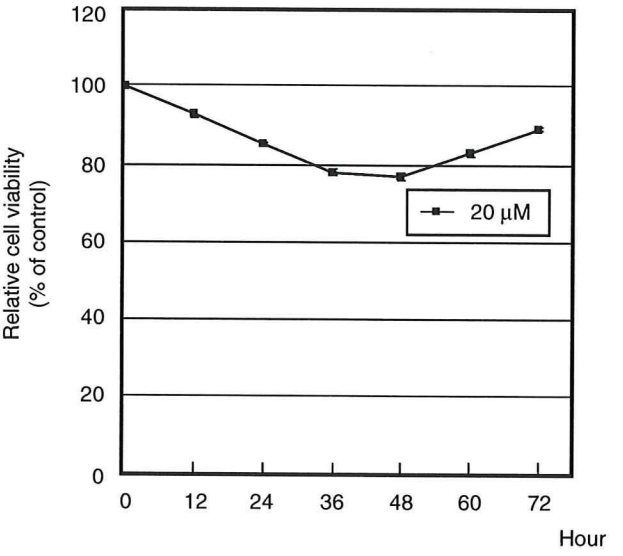

Figure 7 Growth kinetics of griseofulvin treatment of Huh7/Rep-Feo cells. Cells were cultured with [–●–] 20 μM griseofulvin, and cell viability was monitored by a 5-(3-carboxymethoxyphenyl)-2-(4,5-dimethylthiazoly)-3-(4-sulfophenyl) tetrazolium inner salt assay at the times indicated. Error bars indicate mean ± SD.

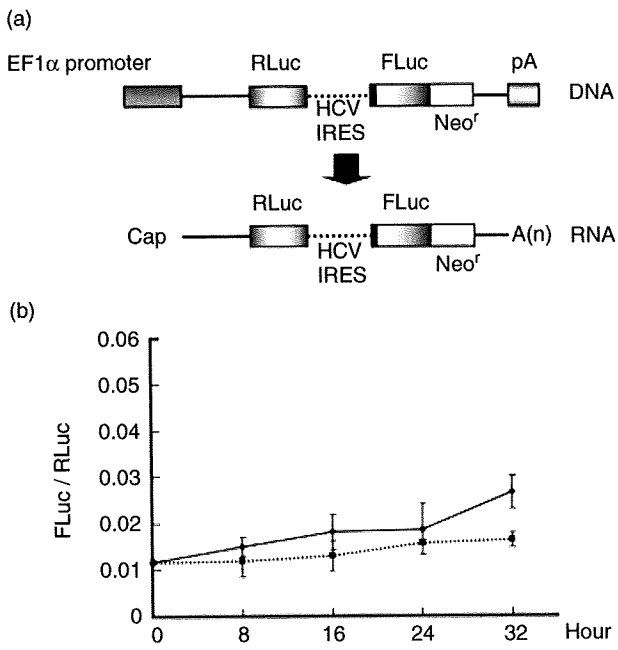

Figure 8 Griseofulvin does not influence hepatitis C virus (HCV) internal ribosomal entry site (IRES)-mediated translation. (a) Structure of the plasmid, pEF-Rluc-HCV IRES Feo. Transcription is initiated under the control of a composite elongation factor 1α (EF1α) promoter. Upstream cistron encodes Renilla luciferase (RLuc) and is translated by a cap-dependent mechanism in transfected cells, while the downstream cistron encodes a fusion (Feo) of the firefly luciferase (Fluc) and neomycin phosphotransferase (Neo^r) genes, translated under the control of the HCV IRES. (b) pEF-Rluc-HCV IRES Feo was stably transfected into Huh7 cells. Cells were treated without (control -◆-) and with 20 μM griseofulvin -■-. Dual luciferase activities were measured at the indicated time points after exposure to griseofulvin. Values are displayed as ratios of Fluc to Rluc. Error bars indicate mean ± SD.

HCV replication, but not HCV IRES-dependent translation.[25] Therefore, we determined whether G_2/M cell cycle arrest by griseofulvin affects HCV IRES-dependent translation using Huh7 cells transfected with pEF Rluc-HCV IRES Feo (Fig. 8a). The treatment of these cells with 20 μM griseofulvin resulted in no significant change of the internal luciferase activities, a concentration that suppressed the expression of the HCV replicon and arrested the HCV replicon cells in the G_2/M phase (Fig. 8b). These results suggested that cell cycle arrest by griseofulvin did not affect HCV IRES-dependent translation, as shown previously for vinblastine sulfate and nocodazole.

Griseofulvin suppressed JFH-1 HCV replication

The studies described thus far were carried out using the subgenomic HCV-1b replicon system. Recently, Wakita *et al.* established a cell culture model for HCV. This system, known as the JFH-1 system and based on genotype 2a HCV, allows the production of a virus that can be efficiently propagated in cell culture (HCVcc).[10] Therefore, we examined the effect of griseofulvin using the JFH-1 system. The Huh7.5.1/JFH-1 cells (cells persistently infected with HCV JFH-1) were cultured with 10 μM or 20 μM griseofulvin for 72 h. We detected the HCV NS3 protein in Huh7.5.1/JFH-1 HCV cells by immunostaining. As shown in Figure 9, in the absence of griseofulvin treatment, the NS3 protein was localized predominantly in the perinuclear region. After treatment of griseofulvin, the NS3 protein expression level was reduced substantially (Fig. 9). This result indicates that griseofulvin also suppresses HCV replication in the JFH-1 HCVcc system.

DISCUSSION

WE HAVE SHOWN here that griseofulvin inhibits the replication of HCV in the HCV subgenomic replicon cells, Huh7/Rep-Feo. In this reporter-based subgenomic replicon system, the EC_{50} of griseofulvin for the inhibition of HCV replication, determined by measurement of the luciferase activity, was approximately 6.13 μM. The real-time RT–PCR and Western blot analyses revealed that both RNA synthesis and its translation were inhibited by griseofulvin in a dose-dependent manner. The treatment of Huh7/Rep-Feo cells with griseofulvin did not activate the IFN inducible gene responses, suggesting that the inhibitory mechanism of griseofulvin in HCV replication is independent of the IFN signaling pathway. Moreover, we demonstrated that the combination treatment of griseofulvin and IFNα had a synergistic inhibitory effect in Huh7/Rep-Feo cells. We also demonstrated that griseofulvin suppressed replication of JFH-1 HCV.

A previous study demonstrated that griseofulvin induces G_2/M arrest in several human cell lines.[24] Here, we show that griseofulvin arrested the Huh7/Rep-Feo cells in the G_2/M phase. Recently, several studies have shown a correlation between HCV IRES-mediated translation and the cell cycle. Honda *et al.* reported that the HCV IRES activity was highest in the G_2/M phase.[26] In contrast, Venkatesan *et al.* reported that the HCV IRES activity was lowest in the G_2/M,[27] while other studies

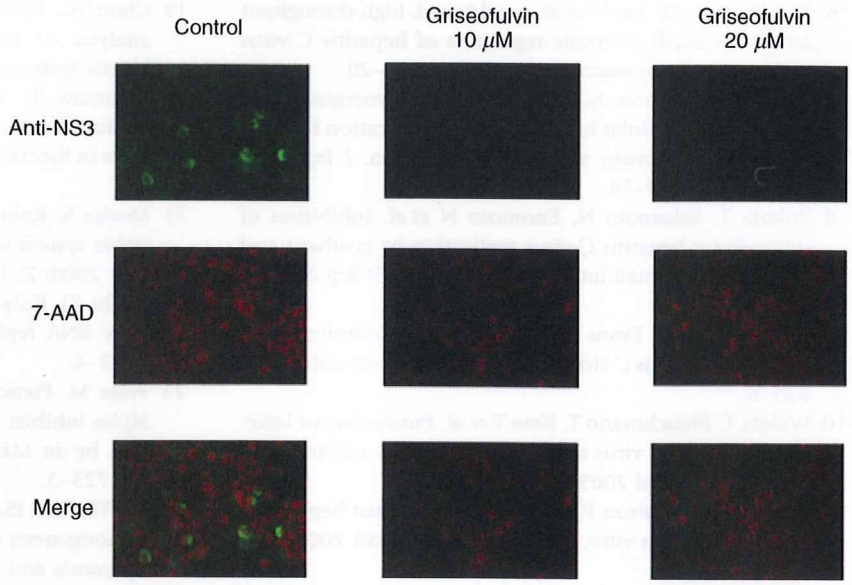

Figure 9 Griseofulvin suppresses JFH-1 replication. Immunofluorescent staining of Huh7.5.1/JFH-1 cells treated with various concentrations of griseofulvin. Hepatitis C virus NS3 protein is stained green and nuclei are stained with 7-aminoactinomycin D (7-AAD; red).

reported that the HCV IRES activity was independent of the stage of the cell cycle.[28,29] In addition, Bost *et al.* reported that several cell cycle inhibitors (vinblastine sulfate, colchicine, nocodazole, and cytochalasin D) did not affect HCV IRES-dependent translation.[25] We also have shown that cell cycle arrest by griseofulvin did not affect HCV IRES-dependent translation. Accordingly, our results support the hypothesis that the HCV IRES activity is independent of the cell cycle.

Previous studies have demonstrated that vinblastine sulfate and nocodazole, well-characterized inhibitors of microtubule polymerization, are able to inhibit HCV-RNA replication in HCV subgenomic replicon cells.[25] These findings indicate that microtubule polymerization is required for the formation of the HCV replication complex. Griseofulvin has been shown to arrest human cells in the G_2/M phase by acting on microtubule polymerization.[30] Thus it is speculated that the inhibition of microtubule polymerization by griseofulvin may influence the formation of the HCV-RNA replication complex. Further, defining the mechanism of action of griseofulvin against HCV replication may be important for defining a novel target for anti-HCV therapy.

Griseofulvin has been used for many years for the treatment of ringworm and other dermatophyte infections. Moreover, griseofulvin does not have significant toxicity for humans. Consequently, the development of derivatives of this compound may be a useful strategy for future therapeutic intervention in chronic hepatitis C.

ACKNOWLEDGMENTS

WE THANK DR Toshio Kitamura (University of Tokyo, Tokyo, Japan) for kindly providing the pGag-pol-IRES-bs^r and pMXs-IN plasmids; Dr Francis V Chisari (The Scripps Research Institute, La Jolla, CA, USA) for kindly providing the Huh7.5.1 cell line; Dr Iyoko Katoh for helpful comments and discussion; and Mr Masashi Osano and Ms Ikuko Kayama (University of Yamanashi, Yamanashi, Japan) for technical assistance. This study was supported by a grant of Health Science from the Ministry of Health, Labor, and Welfare of Japan, and by a grant from the Human Sciences Foundation.

REFERENCES

1 Alter HJ, Purcell RH, Shih JW *et al.* Detection of antibody to hepatitis C virus in prospectively followed transfusion recipients with acute and chronic non-A, non-B hepatitis. *N Engl J Med* 1989; **321**: 1494–500.
2 Choo QL, Kuo G, Weiner AJ *et al.* Isolation of a cDNA clone derived from a blood-borne non-A, non-B viral hepatitis genome. *Science* 1989; **244**: 359–62.
3 Alter MJ. Epidemiology of hepatitis C. *Hepatology* 1997; **26**: 62S–5S.
4 Fried MW, Shiffman ML, Reddy KR *et al.* Peginterferon alfa-2a plus ribavirin for chronic hepatitis C virus infection. *N Engl J Med* 2002; **347**: 975–82.
5 Lohmann V, Korner F, Koch J *et al.* Replication of subgenomic hepatitis C virus RNAs in a hepatoma cell line. *Science* 1999; **285**: 110–13.

6 Kim SS, Peng LF, Lin W *et al.* A cell-based, high-throughput screen for small molecule regulators of hepatitis C virus replication. *Gastroenterology* 2007; **132**: 311–20.
7 Tanabe Y, Sakamoto N, Enomoto N *et al.* Synergistic inhibition of intracellular hepatitis C virus replication by combination of ribavirin and interferon- alpha. *J Infect Dis* 2004; **189**: 1129–39.
8 Yokota T, Sakamoto N, Enomoto N *et al.* Inhibition of intracellular hepatitis C virus replication by synthetic and vector-derived small interfering RNAs. *EMBO Rep* 2003; **4**: 602–8.
9 Lindenbach BD, Evans MJ, Syder AJ *et al.* Complete replication of hepatitis C virus in cell culture. *Science* 2005; **309**: 623–6.
10 Wakita T, Pietschmann T, Kato T *et al.* Production of infectious hepatitis C virus in tissue culture from a cloned viral genome. *Nat Med* 2005; **11**: 791–6.
11 Zhong J, Gastaminza P, Cheng G *et al.* Robust hepatitis C virus infection in vitro. *Proc Natl Acad Sci USA* 2005; **102**: 9294–9.
12 Hinrichsen H, Benhamou Y, Wedemeyer H *et al.* Short-term antiviral efficacy of BILN 2061a hepatitis C virus serine protease inhibitor, in hepatitis C genotype 1 patients. *Gastroenterology* 2004; **127**: 1347–55.
13 Lamarre D, Anderson PC, Bailey M *et al.* An NS3 protease inhibitor with antiviral effects in humans infected with hepatitis C virus. *Nature* 2003; **426**: 186–9.
14 Reesink HW, Zeuzem S, Weegink CJ *et al.* Rapid decline of viral RNA in hepatitis C patients treated with VX-950: a phase Ib, placebo-controlled, randomized study. *Gastroenterology* 2006; **131**: 997–1002.
15 Sarrazin C, Rouzier R, Wagner F *et al.* SCH 503034, a novel hepatitis C virus protease inhibitor, plus pegylated interferon alpha-2b for genotype 1 nonresponders. *Gastroenterology* 2007; **132**: 1270–8.
16 Amemiya F, Maekawa S, Itakura Y *et al.* Targeting lipid metabolism in the treatment of hepatitis C. *J Infect Dis* 2008; **197**: 361–70.
17 Martell M, Gomez J, Esteban JI *et al.* High-throughput real-time reverse transcription-PCR quantitation of hepatitis C virus RNA. *J Clin Microbiol* 1999; **37**: 327–32.
18 Okada Y, Osada M, Kurata S *et al.* p53 gene family p51 (p63) -encoded, secondary transactivator p51B (TAp63alpha) occurs without forming an immunoprecipitable complex with MDM2, but responds to genotoxic stress by accumulation. *Exp Cell Res* 2002; **276**: 194–200.
19 Chou TC, Talaly P. A simple generalized equation for the analysis of multiple inhibitions of Michaelis–Menten kinetic systems. *J Biol Chem* 1977; **252**: 6438–42.
20 Kitamura T, Koshino Y, Shibata F *et al.* Retrovirus-mediated gene transfer and expression cloning: powerful tools in functional genomics. *Exp Hematol* 2003; **31**: 1007–14.
21 Morita S, Kojima T, Kitamura T. Plat-E: an efficient and stable system for transient packaging of retroviruses. *Gene Ther* 2000; **7**: 1063–6.
22 Blight KJ, Kolykhalov AA, Rice CM. Efficient initiation of HCV RNA replication in cell culture. *Science* 2000; **290**: 1972–4.
23 Frese M, Pietschmann T, Moradpour D *et al.* Interferon-alpha inhibits hepatitis C virus subgenomic RNA replication by an MxA-independent pathway. *J Gen Virol* 2001; **82**: 723–3.
24 Ho YS, Duh JS, Jeng JH *et al.* Griseofulvin potentiates antitumorigenesis effects of nocodazole through induction of apoptosis and G2/M cell cycle arrest in human colorectal cancer cells. *Int J Cancer* 2001; **91**: 393–401.
25 Bost AG, Venable D, Liu L *et al.* Cytoskeletal requirements for hepatitis C virus (HCV) RNA synthesis in the HCV replicon cell culture system. *J Virol* 2003; **77**: 4401–8.
26 Honda M, Kaneko S, Matsushita E *et al.* Cell cycle regulation of hepatitis C virus internal ribosomal entry site-directed translation. *Gastroenterology* 2000; **118**: 152–62.
27 Venkatesan A, Sharma R, Dasgupta A. Cell cycle regulation of hepatitis C and encephalomyocarditis virus internal ribosome entry site-mediated translation in human embryonic kidney 293 cells. *Virus Res* 2003; **94**: 85–95.
28 Nelson HB, Tang H. Effect of cell growth on hepatitis C virus (HCV) replication and a mechanism of cell confluence-based inhibition of HCV RNA and protein expression. *J Virol* 2006; **80**: 1181–90.
29 Scholle F, Li K, Bodola F, Ikeda M *et al.* Virus–host cell interactions during hepatitis C virus RNA replication: impact of polyprotein expression on the cellular transcriptome and cell cycle association with viral RNA synthesis. *J Virol* 2004; **78**: 1513–24.
30 Panda D, Rathinasamy K, Santra MK *et al.* Kinetic suppression of microtubule dynamic instability by griseofulvin: implications for its possible use in the treatment of cancer. *Proc Natl Acad Sci USA* 2005; **102**: 9878–83.

doi:10.1111/j.1440-1746.2007.05076.x

HEPATOLOGY

Inhibition of hepatitis C virus infection and expression *in vitro* and *in vivo* by recombinant adenovirus expressing short hairpin RNA

Naoya Sakamoto,*,† Yoko Tanabe,* Takanori Yokota,‡ Kenichi Satoh,§ Yuko Sekine-Osajima,* Mina Nakagawa,*,† Yasuhiro Itsui,* Megumi Tasaka,* Yuki Sakurai,* Chen Cheng-Hsin,* Masahiko Yano,¶ Shogo Ohkoshi,¶ Yutaka Aoyagi,¶ Shinya Maekawa,†† Nobuyuki Enomoto,†† Michinori Kohara§ and Mamoru Watanabe*

Departments of *Gastroenterology and Hepatology, †Hepatitis Control, and ‡Neurology and Neurological Science, Tokyo Medical and Dental University, §Department of Microbiology and Cell Biology, The Tokyo Metropolitan Institute of Medical Science, Tokyo, ¶Gastroenterology and Hepatology Division, Graduate School of Medical and Dental Sciences, Niigata University, Niigata, and ††First Department of Medicine, Yamanashi University, Yamanashi, Japan

Key words
adenovirus vector, hepatitis C virus, RNA interference.

Accepted for publication 12 April 2007.

Correspondence
Dr Naoya Sakamoto, Department of Gastroenterology and Hepatology, Tokyo Medical and Dental University, 1-5-45 Yushima, Bunkyo-ku, Tokyo 113-8519, Japan.
Email: nsakamoto.gast@tmd.ac.jp

NS and YT have contributed equally to this paper.

Abstract

Background and Aim: We have reported previously that synthetic small interfering RNA (siRNA) and DNA-based siRNA expression vectors efficiently and specifically suppress hepatitis C virus (HCV) replication *in vitro*. In this study, we investigated the effects of the siRNA targeting HCV-RNA *in vivo*.

Methods: We constructed recombinant retrovirus and adenovirus expressing short hairpin RNA (shRNA), and transfected into replicon-expressing cells *in vitro* and transgenic mice *in vivo*.

Results: Retroviral transduction of Huh7 cells to express shRNA and subsequent transfection of an HCV replicon into the cells showed that the cells had acquired resistance to HCV replication. Infection of cells expressing the HCV replicon with an adenovirus expressing shRNA resulted in efficient vector delivery and expression of shRNA, leading to suppression of the replicon in the cells by $\sim 10^{-3}$. Intravenous delivery of the adenovirus expressing shRNA into transgenic mice that can be induced to express HCV structural proteins by the Cre/*lox*P switching system resulted in specific suppression of virus protein synthesis in the liver.

Conclusion: Taken together, our results support the feasibility of utilizing gene targeting therapy based on siRNA and/or shRNA expression to counteract HCV replication, which might prove valuable in the treatment of hepatitis C.

Introduction

Hepatitis C virus (HCV), which affects 170 million people worldwide, is one of the most important pathogens causing liver-related morbidity and mortality.[1] The difficulty in eradicating HCV is attributable to limited treatment options against the virus and their unsatisfactory efficacies. Even with the most effective regimen with pegylated interferon (IFN) and ribavirin in combination, the efficacies are limited to less than half of the patients treated.[2] Given this situation, the development of safe and effective anti-HCV therapies is one of our high-priority goals.

RNA interference (RNAi) is a process of sequence-specific, post-transcriptional gene silencing that is initiated by double-stranded RNA.[3,4] Because of its potency and specificity, RNAi rapidly has become a powerful tool for basic research to analyze gene functions and for potential therapeutic applications. Recently, successful suppression of various human pathogens by RNAi have been reported, including human immunodeficiency viruses,[5,6] poliovirus,[7] influenza virus,[8] severe acute respiratory syndrome (SARS) virus[9] and hepatitis B virus (HBV).[10–13]

We and other researchers have reported that appropriately designed small interfering RNA (siRNA) targeting HCV genomic RNA can efficiently and specifically suppress HCV replication *in vitro*.[14–19] We have tested siRNA designed to target the well-conserved 5′-untranslated region (5′-UTR) of HCV-RNA, and identified the most effective target, just upstream of the translation initiation codon. Furthermore, transfection of DNA-based vectors expressing siRNA was as effective as that of synthetic siRNA in suppressing HCV replication.[14]

In this study, we explored the further possibility that efficient delivery and expression of siRNA may be effective in suppression and elimination of HCV replication and that delivery of such

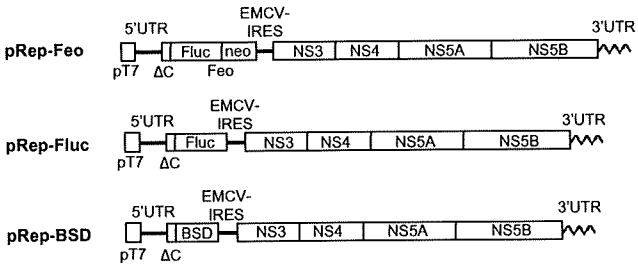

Figure 1 Structures of HCV replicon plasmids. The pRep-Feo expressed a chimeric reporter protein of firefly luciferase (Fluc) and neomycin phosphotransferase (GenBank accession No. AB119282).[14,20] The pRep-Fluc expressed the Fluc protein. The pRep-BSD expressed the blasticidin S (BSD) resistance gene. pT7, T7 promoter; 5'UTR, HCV 5'-untranslated region; ΔC, truncated HCV core region (nt. 342–377); neo, neomycin phosphotransferase gene; EMCV, encephalomyocarditis virus; NS3, NS4, NS5A and NS5B, genes that encode HCV non-structural proteins; 3'UTR, HCV 3'-untranslated region.

HCV-directed siRNA *in vivo* may be effective in silencing viral protein expression in the liver. Here, we report that HCV replication was suppressed *in vitro* by recombinant retrovirus and adenovirus vectors expressing short hairpin RNA (shRNA) and that the delivery of the adenovirus vector to mice *in vivo* specifically inhibited viral protein synthesis in the liver.

Methods

Cells and cell culture

Huh7 and Retro Pack PT67 cells (Clontech, Palo Alto, CA, USA) were maintained in Dulbecco's modified minimal essential medium (Sigma, St. Louis, MO, USA) supplemented with 10% fetal calf serum at 37°C under 5% CO_2. To maintain cell lines carrying the HCV replicon, G418 (Wako, Osaka, Japan) was added to the culture medium to a final concentration of 500 μg/mL.

HCV replicon constructs and transfection

HCV replicon plasmids, pRep-Feo, pRep-Fluc and pRep-BSD were constructed from were constructed from a virus, HCV-N strain, genotype 1b.[21] The pRep-Feo expressed a chimeric reporter protein of firefly luciferase (Fluc) and neomycin phosphotransferase.[14,20] The pRep-Fluc and the pRep-BSD expressed the Fluc and blasticidin S (BSD) resistance genes, respectively (Fig. 1). The replicon RNA synthesis and the transfection protocol have been described previously.[22]

Synthetic siRNA and siRNA-expression plasmid

The design and construction of HCV-directed siRNA vectors have been described.[14] Briefly, five siRNA targeting the 5'-UTR of HCV RNA were tested for their efficiency to inhibit HCV replication, and the most effective sequence, which targeted nucleotide position of 331 though 351, was used in the present study. To construct shRNA-expressing DNA cassettes, oligonucleotide inserts were synthesized that contained the loop sequence (5'-TTC AAG AGA-3') flanked by sense and antisense siRNA sequences (Fig. 2a). These were inserted immediately downstream of the human U6 promoter. To avoid a problem in transcribing shRNA because of instability of the DNA strands arising from the tight palindrome structure, several C-to-T point mutations, which retained completely the silencing activity of the shRNA, were introduced into the sense strand of the shRNA sequences (referred to as 'm').[23] A control plasmid, pUC19-shRNA-Control, expressed shRNA directed towards the Machado–Joseph disease gene, which is a mutant of ataxin-3 gene and is not normally expressed. We have previously described the sequence specific activity of the shRNA-Control.[24]

Prior to construction of the virus vectors, we tested silencing efficiency of five shRNA constructs of different lengths that covered the target sequence (Fig. 2a). The shRNA-HCV-19, shRNA-HCV-21 and shRNA-HCV-27 had target sequences of 19, 21 and 27 nucleotides, respectively. Transfection of these shRNA constructs into Huh7/pRep-Feo showed that shRNA with longer target sequences had better suppressive effects (Fig. 2b). Therefore, we used shRNA-HCV-27m (abbreviated as shRNA-HCV) in the following study.

Recombinant retrovirus vectors

The U6-shRNA expression cassettes were inserted into the *StuI*/*Hin*dIII site of a retrovirus vector, pLNCX2 (Clontech) to construct pLNCshRNA-HCV and pLNCshRNA-Control (Fig. 2c). The plasmids were transfected into the packaging cells, Retro Pack PT67. The culture supernatant was filtered and added onto Huh7 cells with 4 μg/mL of polybrene. Huh7 cell lines stably expressing shRNA were established by culture in the presence of 500 μg/mL of G418.

Recombinant adenovirus

Recombinant adenoviruses expressing shRNA were constructed using an Adenovirus Expression Vector Kit (Takara, Otsu, Japan). The U6-shRNA expression DNA cassette was inserted into the *Swa*I site of pAxcw to construct pAxshRNA-HCV and pAxshRNA-Control. The adenoviruses were propagated according to the manufacturer's protocol (AxshRNA-HCV and AxshRNA-Control; Fig. 2c). A 'multiplicity of infection' (MOI) was used to standardize infecting doses of adenovirus. The MOI stands for the ratio of infectious virus particles to the number of cells being infected. An MOI = 1 represents equivalent dose to introduce one infectious virus particle to every host cell that is present in the culture.

Plasmids for assays of interferon responses

pISRE-TA-Luc (Invitrogen, Carlsbad, CA, USA) contained five copies of the consensus interferon stimulated response element (ISRE) motifs upstream of the Fluc gene. pTA-Luc (Invitrogen), which lacks the enhancer element, was used for background determination. The pcDNA3.1 (Invitrogen) was used as an empty vector for mock transfection. pRL-CMV (Promega, Madison, WI, USA), which expresses the *Renilla* luciferase protein, was used for normalization of transfection efficiency.[25] A plasmid, peGFPneo (Invitrogen), was used to monitor percentages of transduced cells.

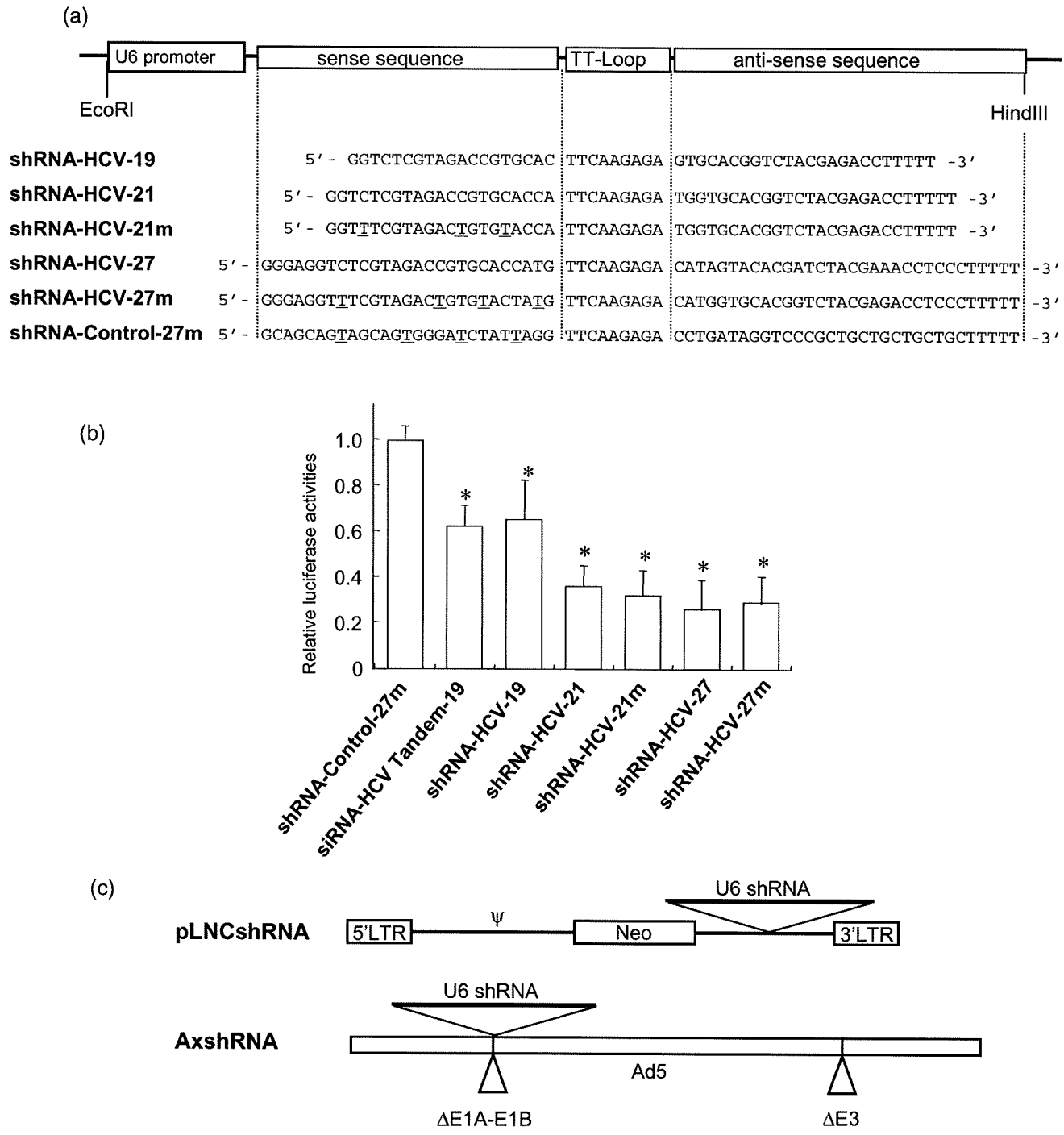

Figure 2 Structure of shRNA-expression constructs and shRNA sequences. (a) Structure of shRNA-expression cassette and shRNA sequences. TT-Loop, the loop sequence. The shRNA-Control was directed toward an unrelated target, Machado–Joseph disease gene. Underlined letters indicate C-to-T point mutations in the sense strand. (b) The shRNA-expression plasmids were transfected into Huh7/pRep-Feo cells, and internal luciferase activities were measured at 48 h of transfection. Each assay was done in triplicate, and the values are displayed as mean + SD. $*P < 0.05$. (c) pLNCshRNA, structure of a recombinant retrovirus expressing shRNA. Ψ, the retroviral packaging signal sequence. AxshRNA, structure of a recombinant adenovirus expressing shRNA.

Real-time RT-PCR analysis

Total cellular RNA was extracted from cultured cells or liver tissue using ISOGEN (Nippon Gene, Tokyo, Japan). Total cellular RNA (2 μg) was used to generate cDNA from each sample using the SuperScript II reverse-transcriptase (Invitrogen). The mRNA expression levels were measured using the Light Cycler PCR and detection system (Roche, Mannheim, Germany) and Light Cycler Fast Start DNA Master SYBR Green 1 mix (Roche).

Luciferase assays

Luciferase activity was measured using a luminometer, Lumat LB9501 (Promega) and the Bright-Glo Luciferase Assay System (Promega) or the Dual-Luciferase Reporter Assay System (Promega).

Northern and western hybridization

Total cellular RNA was separated by denaturing agarose-formaldehyde gel electrophoresis, and transferred to a nylon membrane. The membrane was hybridized with a digoxigenin-labeled probe specific for the full-length replicon sequence, and subsequently with a probe specific for beta-actin. The signals were detected by chemiluminescence reaction using a Digoxigenin Luminescent Detection Kit (Roche), and visualized by Fluoro-Imager (Roche). For the western blotting, 10 μg of total cell lysate was separated on NuPAGE 4.12% Bis-TrisGel (Invitrogen), and blotted onto an Immobilon PVDF Membrane (Roche). The membrane was incubated with monoclonal antibodies specific for HCV-NS5A (BioDesign, Saco, ME, USA), NS4A (Virogen, Watertown, MA, USA), or beta-actin (Sigma), and detected by a chemiluminescence reaction (BM Chemiluminescence Blotting Substrate; POD, Roche).

Transient-replication assays

A replicon, pRep-Fluc, was transfected into cells and the luciferase activities of the cell lysates were measured serially. To correct the transfection efficiency, each value was divided by the luciferase activity at 4 h after the transfection.

Stable colony formation assays

Cells were transfected with a replicon, pRep-BSD, and were cultured in the presence of 150 μg/mL of BSD (Invitrogen). BSD-resistant cell colonies appeared after ~3 weeks of culture, and were counted.

HCV-JFH1 virus cell culture

An *in-vitro* transcribed HCV-JFH1 RNA[26] was transfected into Huh7.5.1 cells.[27] Naive Huh7.5.1 cells were subsequently infected by the culture supernatant of the JFH1-RNA transfected Huh-7.5.1 cells, and subjected to siRNA or drug treatments. Replication levels of HCV-RNA were quantified by the realtime RT-PCR by using primers that targeted HCV-NS5B region, HCV-JFH1 sense: 5′-TCA GAC AGA GCC TGA GTC CA-3′, and HCV-JFH1 antisense: 5′-AGT TGC TGG AGG GCT TCT GA-3′.

Mice and adenovirus infection

Transgenic mice, CN2-29, inducibly express mRNA for the HCV structural proteins (genotype1b, nucleotides 294–3435) by the Cre/*lox*P switching system.[28] The transgene does not contain full-length HCV 5′-UTR, but shares the target sequence of the shRNA-HCV. Although the transgenic mouse CN2 has been previously reported as expressing higher levels of the viral proteins, the expression levels of the viral core protein in the CN2-29 mice are modest and similar to that in the liver of HCV patients. Thus, we chose CN2-29 mice in the present study.

The mice were infected with AxshRNA-HCV or controls (AxshRNA-Control or AxCAw1) in combination with AxCAN-Cre, which expressed Cre recombinase. Three days after the infection, the mice were killed and HCV core protein in the liver was measured as described below. The BALB/c mice were maintained in the Animal Care Facility of Tokyo Medial and Dental University, and transgenic mice were in the Tokyo Metropolitan Institute of Medical Science. Animal care was in accordance with institutional guidelines. The review board of the university approved our experimental animal studies and all experiments were approved by the institutional animal study committees.

Measurement of HCV core protein in mouse liver

The amounts of HCV core protein in the liver tissue from the mice was measured by a fluorescence enzyme immunoassay (FEIA)[29] with a slight modification. Briefly, the 5F11 monoclonal anti-HCV-core antibody was used as the first antibody on the solid phase, and the 5E3 antibody conjugated with horseradish peroxidase was the second antibody. This FEIA can detect as little as 4 pg/mL of recombinant HCV-core protein. Contents of the HCV core protein in the liver samples were normalized by the total protein contents and expressed as pg/mg total protein.

Immunohistochemical staining

Liver tissue was frozen with optimal cutting temperature (OTC) compound (Tissue Tek; Sakura Finetechnical, Tokyo, Japan). The sections (8 μm thick) were fixed with a 1:1 solution of acetone : methanol at −20°C for 10 min and then washed with phosphate-buffered saline (PBS). Subsequently, the sections were incubated with the IgG fraction of an anti-HCV core rabbit polyclonal antibody (RR8)[28] in blocking buffer or antialbumin rabbit polyclonal antibody (Dako Cytomation, Glostrup, Denmark) in PBS overnight at 4°C. The sections were incubated with secondary antibody, Alexa-antirabbit IgG (Invitrogen) or TRITIC-antirabbit IgG (Sigma), for 2 h at room temperature. Fluorescence was observed using a fluorescence microscope.

Statistical analyses

Statistical analyses were performed using Student's *t*-test; *P*-values of less than 0.05 were considered to be statistically significant.